GEORGIA INSTITUTE OF TECHNOLOGY
OFFICE OF CONTRACT ADMINISTRATION
SPONSORED PROJECT INITIATION

Date: 1/25/79

Project Title: Measurements of Aerosol Optical Properties as a Part of the GAMETAG Program

Project No: G-35-647 Green card

Project Director: Dr. Gerald W. Grams

Sponsor: National Science Foundation, Washington, D. C. 20550

Agreement Period: From 11/15/78 Until 4/30/80*
*Includes 6 month flexibility period

Type Agreement: Grant No. ATM-7810091 (thru G.I.T.)

Amount: $34,800 NSF Funds (G-35-647)
1,981 GIT Contribution (G-35-334)
$36,781 TOTAL

Reports Required: Annual Progress Reports; Final Project Report

Sponsor Contact Person (s):

Technical Matters
Mr. Ronald C. Taylor
Division of Atmospheric Sciences
National Science Foundation
1800 G Street, N.W.
Washington, D. C. 20550

Phone: (202) 632-4190

Contractual Matters
(thru OCA)

Ms. Lois A. Shapiro
Grants Specialist - Area 4
National Science Foundation
1800 G Street, N.W.
Washington, D. C. 20550
Phone: (202) 632-5884

Defense Priority Rating: n/a

Assigned to: Geophysical Sciences (School/Laboratory)

COPIES TO:

- Project Director
- Division Chief (EES)
- School/Laboratory Director
- Dean/Director–EES
- Accounting Office
- Procurement Office
- Security Coordinator (OCA)
- ✓Reports Coordinator (OCA)
- Library, Technical Reports Section
- EES Information Office
- EES Reports & Procedures
- Project File (OCA)
- Project Code (GTRI)
- Other

CA–3 (3/76)

GEORGIA INSTITUTE OF TECHNOLOGY
OFFICE OF CONTRACT ADMINISTRATION

SPONSORED PROJECT TERMINATION

Date: 1/19/81

Project Title: Measurements of Aerosol Optical Properties as a Part of the GAMETAG Program

Project No: G-35-647

Project Director: Dr. Gerald W. Grams

Sponsor: National Science Foundation, Washington, D.C. 20550
ATM-7810091 (thru G.I.T.)

Effective Termination Date: 4/3/80

Clearance of Accounting Charges: 4/3/80

Grant/Contract Closeout Actions Remaining:

_ Final Invoice and Closing Documents
X Final Fiscal Report
_ Final Report of Inventions
_ Govt. Property Inventory & Related Certificate
_ Classified Material Certificate
_ Other _____

Assigned to: Geophysical Sciences (School/~~Laboratory~~)

COPIES TO:

Project Director
Division Chief (EES)
School/Laboratory Director
Dean/Director–EES
Accounting Office
Procurement Office
Security Coordinator (OCA)
Reports Coordinator (OCA)

Library, Technical Reports Section
EES Information Office
Project File (OCA)
Project Code (GTRI)
Other C.E. Smith

CA–4 (1/79)

G-35-[illegible]

NATIONAL SCIENCE FOUNDATION
Washington, D.C. 20550

FINAL PROJECT REPORT
NSF FORM 98A

PLEASE READ INSTRUCTIONS ON REVERSE BEFORE COMPLETING

PART I–PROJECT IDENTIFICATION INFORMATION

1. Institution and Address	2. NSF Program	3. NSF Award Number
Georgia Institute of Technology School of Geophysical Sciences Atlanta, Georgia 30332	METEOROLOGY	ATM-7810091
	4. Award Period From 11/15/78 To 4/30/80	5. Cumulative Award Amount $34,800

6. Project Title

Measurement of Aerosol Properties as a Part of the GAMETAG Program

PART II–SUMMARY OF COMPLETED PROJECT *(FOR PUBLIC USE)*

The aerosol measurement component of GAMETAG (Global Atmospheric Measurement Experiment on Tropospheric Aerosols and Gases) was designed to provide an initial assessment of concentrations and types of natural airborne aerosol particles in remote locations with an emphasis on determining the optical properties of the particles for use in studies of the effect of the particles on the earth's climate and on atmospheric visibility. The GAMETAG program brought together scientists from universities, government laboratories, and private industry to obtain coordinated observations of the worldwide distribution of atmospheric trace gases and aerosol species. Under this program, simultaneous data were obtained on over 40 different chemical and meteorological variables in the troposphere over both continental and marine environments for geographical locations ranging from Alaska and Northern Canada to the remote regions south of New Zealand. These measurements were made with equipment installed by the scientific investigators on the Lockheed Electra atmospheric research aircraft operated by the National Center for Atmospheric Research. As part of this effort, Georgia Tech's airborne aerosol optics measurement system was installed on the Electra and was operated continuously during the GAMETAG flights. Data obtained with the aerosol optics system, data recorded simultaneously by other investigator's instruments, samples of particles collected on filters and impaction surfaces, and correlative aircraft data were analyzed to determine mass concentrations and to study the composition and optical properties of the aerosols along all the aircraft flight paths. For the continental measurements, particles with diameters less than about 1 micron were dominated by sulfate and combustion aerosols; larger sizes were dominated by crustal particles. The crustal aerosol was shown to be a significant component of the background tropospheric aerosol in western North America with a potentially significant contribution to atmospheric visibility reduction in this region. The Pacific marine measurements showed that the aerosol is dominated by sea spray aerosols near the oceanic surface; at higher altitudes, the measurements showed a highly variable character for the aerosol paricles with large concentration fluctuations within a few kilometers suggesting that mid-tropospheric aerosol populations are significantly influenced by transport from continental areas over large areas of the Pacific.

PART III–TECHNICAL INFORMATION *(FOR PROGRAM MANAGEMENT USES)*

1. ITEM *(Check appropriate blocks)*	NONE	ATTACHED	PREVIOUSLY FURNISHED	TO BE FURNISHED SEPARATELY TO PROGRAM	
				Check (✓)	Approx. Date
a. Abstracts of Theses		X			
b. Publication Citations		X			
c. Data on Scientific Collaborators		X			
d. Information on Inventions	X				
e. Technical Description of Project and Results		X			
f. Other *(specify)*					

2. Principal Investigator/Project Director Name *(Typed)*	3. Principal Investigator/Project Director Signature	4. Date
Prof. Gerald W. Grams		12/17/80

INSTRUCTIONS FOR FINAL PROJECT REPORT
(NSF FORM 98A)

This report is due within 90 days after the expiration of the award. It should be submitted in two copies to:

National Science Foundation
Division of Grants and Contracts
Post-Award Projects Branch
1800 G Street, N.W.
Washington, D.C. 20550

INSTRUCTIONS FOR PART I

These identifying data items should be the same as on the award documents.

INSTRUCTIONS FOR PART II

The summary (about 200 words) must be self-contained and intelligible to a scientifically literate reader. Without restating the project title, it should begin with a topic sentence stating the project's major thesis. The summary should include, if pertinent to the project being described, the following items:

- The primary objectives and scope of the project.
- The techniques or approaches used only to the degree necessary for comprehension.
- The findings and implications stated as concisely and informatively as possible.

This summary will be published in an annual NSF report. Authors should also be aware that the summary may be used to answer inquiries by nonscientists as to the nature and significance of the research. Scientific jargon and abbreviations should be avoided.

INSTRUCTIONS FOR PART III

Items in Part III may, but need not, be submitted with this Final Project Report. Place a check mark in the appropriate block next to each item to indicate the status of your submission.

a. Self-explanatory.
b. For publications (published and planned) include title, journal or other reference, date, and authors. Provide two copies of any reprints as they become available.
c. Scientific Collaborators: provide a list of co-investigators, research assistants and others associated with the project. Include title or status, e.g. associate professor, graduate student, etc.
d. Briefly describe any inventions which resulted from the project and the status of pending patent applications, if any.
e. Provide a technical summary of the activities and results. The information supplied in proposals for further support, updated as necessary, may be used to fulfill this requirement.
f. Include any additional material, either specifically required in the award instrument (e.g. special technical reports or products such as films, books, studies) or which you consider would be useful to the Foundation.

Attachment to NSF Award Form 984 for Project ATM-7810091

a. Proposed M. S. thesis topic for M. Zakikhani, School of Geophysical Sciences, Georgia Tech (initial work supported by above NSF grant).

Title: Models of the optical properties of aerosol particles in the troposphere and lower stratosphere.

Abstract: It is proposed to analyze existing data on aerosol size distributions and phase functions, compare the data set with current aerosol models, and use the data set to refine the aerosol models. There are many applications for data on the optical properties of aerosol particles for calculations of the effect of suspended particulates on climate, for studies of visibility degradation by aerosols, and for general considerations involving the effect of aerosols on propagation of visible and infrared radiation in the atmosphere. Several models have been proposed and used by various investigators but the optical parameters are often based on limited data sets. In several field experiments, members of the Atmospheric Optics Laboratory at Georgia Tech have collected simultaneous data on particle size distributions and scattering phase functions (angular scattering patterns) using instrumentation operated on a long-range Electra aircraft in the troposphere and a high-altitude Sabreliner aircraft in the lower stratosphere. This data will be used to make the intercomparisons with the current aerosol models and will be used as the basis for the refinements to those models.

b. Publication Citations

Patterson, E.M., C.S. Kiang, A.C. Delany, A.F. Wartborg, A.C.D. Leslie, and B.J. Huebert, 1980: Global Measurements of Aerosols in Remote Continental and Marine Regions: Concentrations, Size Distributions, Optical Properties. J. Geophys. Res. (in press)

c. Scientific Collaborators

E. M. Patterson, Research Scientist, School of Geophysical Sciences, Georgia Institute of Technology, Atlanta, GA 30332.

M. Zakikhani, Graduate Research Assistant, School of Geophysical Sciences, Georgia Institute of Technology, Atlanta, GA 30332.

MEASUREMENTS OF AEROSOL OPTICAL PROPERTIES AS A PART OF THE GAMETAG PROGRAM

Final Technical Report
NSF Grant Number ATM-7810091

Principal Investigator

Prof. Gerald W. Grams
School of Geophysical Sciences
Georgia Institute of Technology
Atlanta, Georgia 30332

Introduction

The Global Atmospheric Measurement Experiment of Tropospheric Aerosols and Gases (GAMETAG) had as its objective the coordinated measurement of global distributions of atmospheric trace gases and aerosol particles to obtain an understanding of atmospheric chemical properties and processes. Aerosol measurements in the Phase I GAMETAG program were specifically designed to observe aerosols in both the free troposphere and the planetary boundary layer under a variety of conditions. The measurements were performed to provide a data base for the assessment of causal relationships between observed aerosol distributions and factors controlling aerosol populations and to provide an initial assessment of the optical properties of airborne particulates in remote regions. In order to meet these objectives, the following research tasks were proposed:

- Analysis and interpretation of in-situ size distribution data obtained by single-particle optical counters.
- Analysis of particles collected on nuclepore filters using scanning electron microscopy for determination of elemental composition on a single-particle and total-sample basis.
- Analysis of in-situ polar nephelometer data and of aerosol particles collected on filters during the GAMETAG flights to determine aerosol optical properties.
- Calculations of optical and radiative parameters needed to determine possible effects of the measured aerosol particles on climate or on atmospheric visibility.

Each of the above tasks was accomplished successfully. Our study has, in fact, produced considerably more data than envisioned in our original proposal. With regard to the assessment of aerosol distributions, we analyzed aerosol data for continental and marine aerosols in both the mid-troposphere and the planetary boundary layer to obtain latitudinal profiles of aerosol concentration and extinction for our aircraft flight tracks over the Pacific. Our data on the marine aerosol has been used to address the question of background aerosol characteristics in remote areas of the Pacific for both boundary layer and mid-tropospheric measurements. In addition, our analysis has provided new data concerning possible gas-to-particle conversion processes

in mid-oceanic regions, as well as new data on the scattering properties of aerosol particles along the aircraft flight tracks.

Details of aircraft flight tracks, instrumentation, and data analysis procedures are given in the paper "Global Measurements of Aerosols in Remote Continental and Marine Regions: Concentrations, Size Distributions, Optical Properties" which is attached to this report as an appendix.

Optical Properties of Measured Aerosol Particles

Our polar nephelometer data were obtained to determine aerosol optical properties for use in calculating possible effects of measured aerosol particles on climate or on atmospheric visibility. These observations were made with a laser-based instrument designed to operate in a pressurized aircraft cabin. The instrument samples outside air ducted by an airflow tube through a volume defined by the intersection of a collimated linearly polarized laser beam with the viewing volume of a narrow field-of-view detector system that incorporates a photomultiplier tube. The laser beam is mechanically "chopped" and a two-channel pulse counter, synchronized to the laser output, measures photomultiplier pulse rates with the light both on and off. The difference in the measured pulse rates is directly proportional to the intensity of the light scattered from the particles in the sample volume. The above nephelometer system has been described by Grams, et al. (1975).

Light-scattering measurements were made at scattering angles from 15° to 165° from the direction of propagation of the light beam in 5° steps in the plane that is parallel to the electric vector of the incident polarized laser beam. An example of the nephelometer data is shown in Fig. 1. Data points are plotted as circles; error bars based on observed fluctuations of the signal at each angle over a 10-minute observation period are also plotted.

The solid line in Fig. 1 was obtained by applying a non-linear least-squares procedure (similar to that described by Grams, et al., 1974) for fitting data points to analytic curves using the Henyey-Greenstein phase function,

$$P_{HG}(\theta) = (1 - g^2)/(1 + g^2 - 2g \cos \theta)^{3/2} \qquad (1)$$

to specify the aerosol scattering contributions. In the above expression, θ

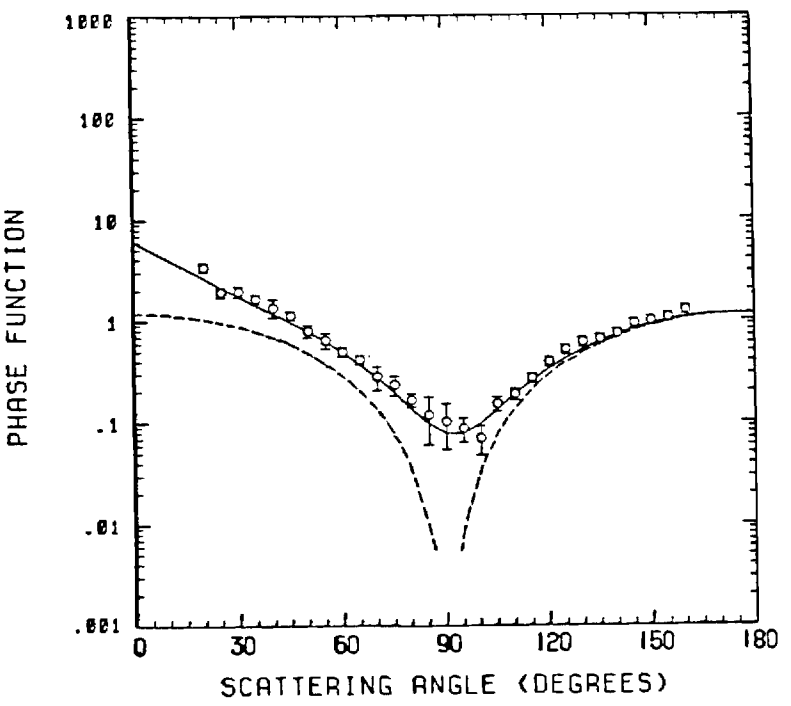

Figure 1
Example of polar nephelometer observations during project GAMETAG. The data were obtained in the marine free troposphere during a flight from San Francisco to Hawaii on April 28, 1978. Circles with error bars are data points; dashed lines are relative contributions to the observed phase functions due to molecular scattering; solid lines represent the phase function for both aerosol and molecular scattering for which the Henyey-Greenstein phase function was used to specify aerosol contributions. Best fit Henyey-Greenstein parameters include an asymmetry factor g=0.66 and aerosol scattering ratio f=0.31.

is the scattering angle and g is the asymmetry parameter (the average over a unit sphere of $\cos\theta$, weighted by the scattering phase function). This expression was introduced many years ago in the astro-physics literature to describe intensity patterns observed for diffuse interstellar radiation (Henyey and Greenstein, 1941). Hansen (1969) demonstrated that $P_{HG}(\theta)$ can be used to replace the more realistic Mie-scattering phase functions in multiple-scattering calculations with no more than a few percent error in computed fluxes.

In earlier polar nephelometer studies, we analyzed simultaneous data on scattering phase functions and particle size distributions to determine best-fit optical parameters such as the imaginary refractive index n_{IM} for Mie scattering theory (e.g., Grams, et al., 1974). However, during the GAMETAG flights, the laser nephelometer was controlled by a minicomputer data recording system and, with the automated operation, we substantially increased the amount of data to process. We therefore began to use the Henyey-Greenstein function to carry out preliminary inspections of our data rather than using the previous analysis procedures which were based on Mie scattering theory and which

consumed significantly more computer time. We found for the conditions of the GAMETAG flights that excellent agreement was obtained using the "best-fit" $P_{HG}(\theta)$ to describe the actual observed phase function $P(\theta)$. We therefore made extensive use of the results of our comparisons with the Henyey-Greenstein equation to specify realistic scattering phase functions for applications such as aerosol-climate models.

The ability to specify analytic functions for $P(\theta)$ is of considerable interest in aerosol-climate studies since the use of parameters based on real data rather than calculated angular scattering function eliminates a variety of critical questions related to the basic assumptions (e.g., spherical shapes and uniform particle composition) for using Mie scattering theory to calculate aerosol optical parameters from observed particle size distributions and bulk optical properties (Grams, 1980). Particle shape and composition is so varied in the atmosphere that effects of nonspherical particle shapes and/or non-uniform particle composition must always be addressed in models of the radiative effects of airborne particulates. Thus, an ability to obtain a direct in-situ measurement of the aerosol-scattering phase function without reference to particle size, shape, or composition for direct use in models of the radiative effects of aerosol particles eliminates the uncertainties associated with effects of nonspherical particle shape and non-uniform particle composition on the phase functions used in the model.

As a specific example of how our scattering data can be applied, we point out that many of the published models of the radiative effects of aerosol particles are able to calculate net changes in the vertical flux of terrestrial radiation due to the presence of aerosol particles from three basic optical parameters: the optical thickness τ, the single-scattering ableda ω, and the scattering phase function $P(\theta)$ for the aerosol particles. As discussed above, the Georgia Tech polar nephelometer provides in-situ data on $P(\theta)$; furthermore, its observations of scattering intensity versus scattering angle can be integrated over angle to obtain the aerosol scattering coefficient per unit volume $\sigma_{SCA}[cm^2/cm^3]$. While data on $P(\theta)$ and σ_{SCA} alone would have some limited value for defining aerosol optical parameters, the advantages of the GAMETAG approach of obtaining simultaneous data with other instruments on the same aircraft platform is demonstrated by the fact that in-situ

PMS* aerosol data can be used to compute aerosol extinction coefficients $\sigma_{EXT}[cm^2/cm^3]$. This parameter is calculated by applying Mie scattering theory to particle size distributions determined by the PMS counters for representative values of the aerosol complex refractive index obtained from studies of filter samples collected during the GAMETAG flights, as described in the appendix. Even though calculations of $P(\theta)$ and σ_{SCA} would be significantly affected by variations in the complex refractive index of the airborne particulates (Grams, et al., 1974), σ_{EXT} is relatively insensitive to such refractive index changes (Patterson, et al., 1976). Combining the in-situ data from the PMS aerosol spectrometer data thereby provides enough information to completely specify each of the three basic optical parameters needed to estimate possible effects of the measured aerosol particles on the earth's radiation balance. The optical thickness τ is simply the integral over appropriate optical paths of the σ_{EXT} values calculated from the PMS data. With σ_{SCA} values obtained by integrating polar nephelometer light-scattering intensities over angles, the single-scattering albedo is the ratio $\omega = \sigma_{SCA}/\sigma_{EXT}$. The $P(\theta)$ values, of course, are measured directly by the polar nephelometer.

Fig. 2 shows average values of aerosol extinction σ_{EXT} along our Pacific flight tracks for marine free troposphere (MFT) observations. Marine boundary layer (MBL) observations show average extinction cross sections of $\sim 10^{-7}$/cm: our MFT data show average extinctions ranging from about 2×10^{-9}/cm south of 20°S to over 2×10^{-8}/cm north of 20°N. This range of variability of σ_{EXT} values was also displayed by the polar nephelometer observations. The "best-fit" Henyey-Greenstein parameters in Fig. 1 include the asymmetry factor $g = 0.66$ and the aerosol scattering ratio $f = 0.31$ (i.e., σ_{SCA} is 31% of the molecular scattering cross section). Fig. 3 shows a polar scattering diagram for MFT conditions on the southernmost portion of the 1978 GAMETAG flights. With "best-fit" Henyey-Greenstein parameters of $g \approx 0$ (indicating very small particle sizes) and $f = 0.06$ (aerosol scattering only 6% of molecular scattering), the light-scattering data from the southernmost parts of the GAMETAG flights are consistent with the extremely small extinction coefficients

*Particle Measurement Systems, Inc., single-particle optical counters operated by A. Delany of NCAR on the Electra aircraft to provide aerosol particle size spectra during the GAMETAG flights.

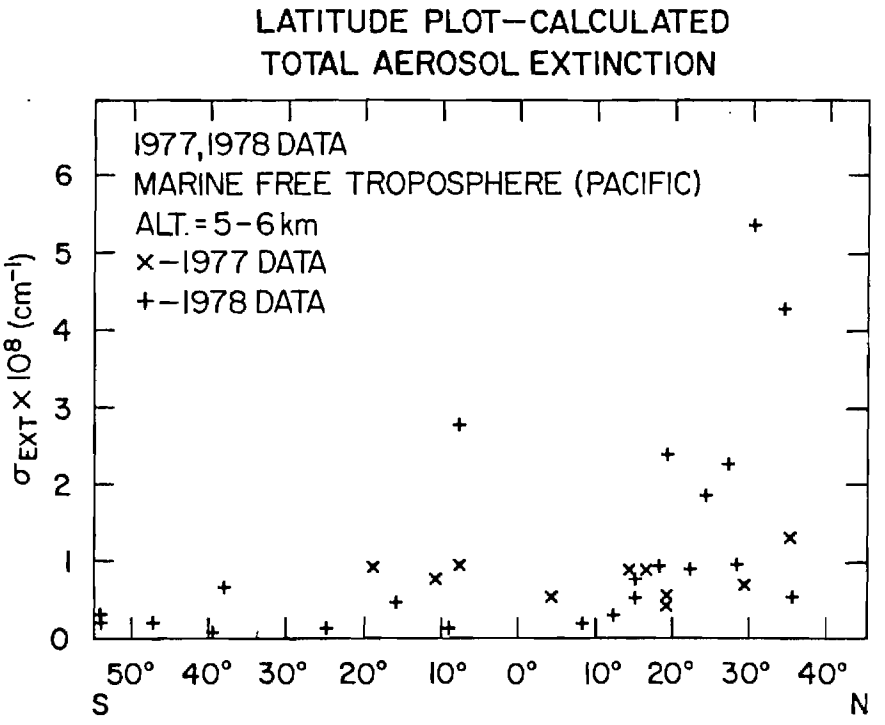

Figure 2

Calculated optical extinction for 1977 (x) and 1978 (+) GAMETAG marine free troposphere data plotted as a function of latitude along the Pacific flight tracks.

Figure 3

As in Figure 2 except for data taken in the marine free troposphere on May 10, 1978, during a round-trip flight from Christchurch, New Zealand, southward to 58°S and back. This phase function data indicates extremely clean air with an aerosol scattering ratio of f=0.057 and an asymmetry factor g of almost zero suggesting very small particle sizes (see text for more details).

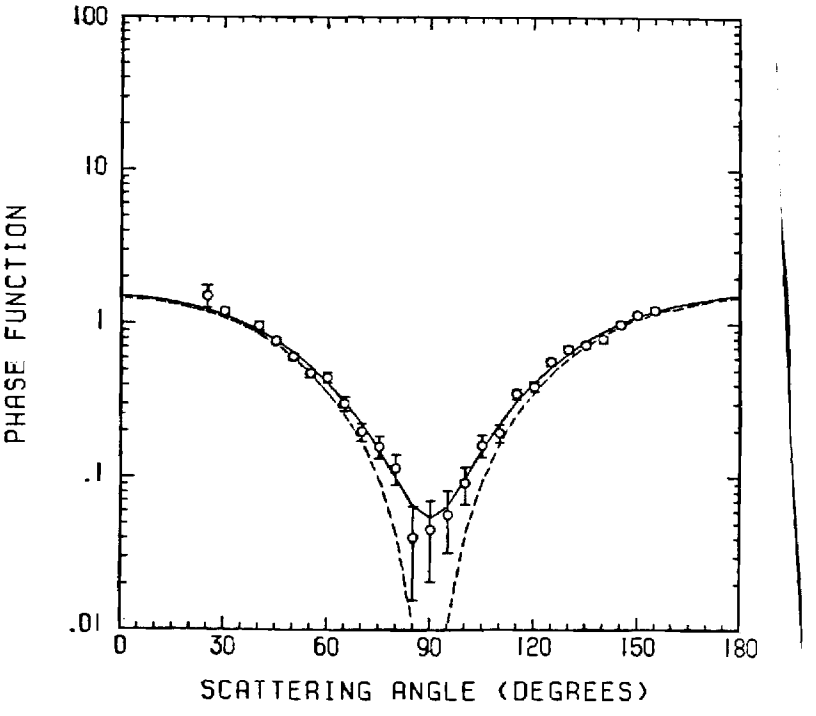

indicated on the left side of Fig. 2.

We have compared ratios, f_{SCA}, of aerosol scattering to molecular scattering obtained from our polar nephelometer studies and extinction ratios, f_{EXT}, calculated from the observations. To illustrate the amount and the quality of data we have on these parameters, Fig. 4 shows values of f_{SCA}

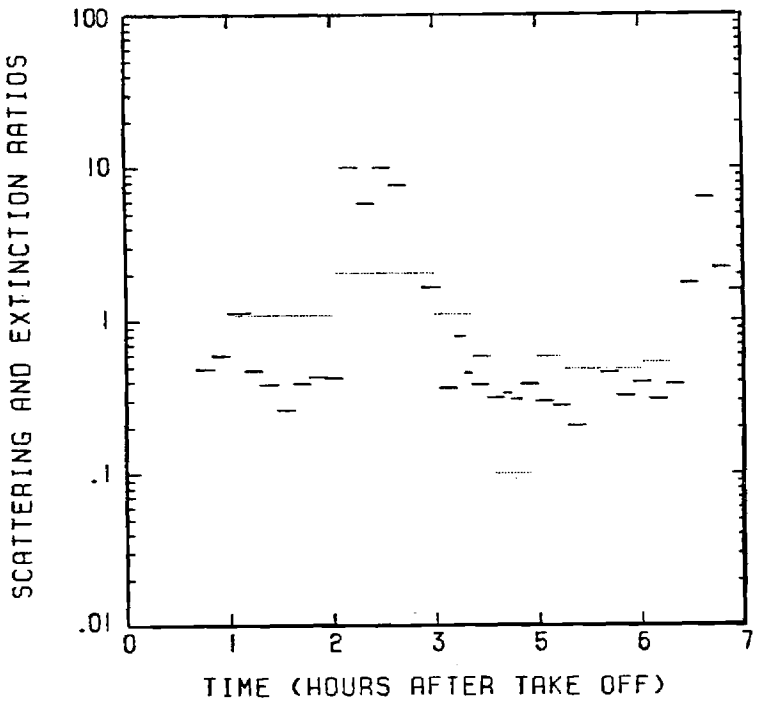

Figure 4

A comparison of aerosol extinction ratios, f_{EXT}, inferred from the PMS optical particle counter observations (....) and the aerosol scattering ratios, f_{SCA} determined from the polar nephelometer observations (____). The results are plotted versus the time in flight for the 1978 Electra GAMETAG flight from San Francisco to Hilo, Hawaii.

obtained from the polar nephelometer data (solid lines) and f_{EXT} obtained from the PMS particle size distributions (dashed lines) for a 1978 Electra GAMETAG flight from San Francisco to Hilo, Hawaii. The length of time for each measurement is indicated by the horizontal length of each data line. While these results must be regarded as preliminary in nature, it is clear that good possibilities also exist for inferring values of the single scattering albedos from such data ($\omega = \sigma_{SCA}/\sigma_{EXT} = f_{SCA}/f_{EXT}$).

A detailed analysis of the scattering data forms part of the M.S. thesis project of a student whose initial support was provided by this grant. This project involves the use of the GAMETAG data and other observations made with the polar nephelometer and various particle size spectrometers on the NCAR Sabreliner during November 1978 and July 1979. (The expected date for completion of this study is Spring 1981.) The above thesis project is part

of a continuing effort at Georgia Tech to determine the validity of existing models for calculating the radiative effects of stratospheric and tropospheric aerosol particles on the climate or on atmospheric visibility. In conjunction with an on-going laboratory program (Grams, 1980) for studying the effects of particle characteristics that deviate from those assumed by the Mie theory for calculating light-scattering by small particles, we expect to be able to develop improved models for use in radiative transfer calculations.

Concentration Levels and Characteristics for Continental and Marine Aerosols

In addition to the optical studies summarized above, we also used the PMS optical particle counter data, elemental and ionic composition information, and particle morphology to characterize physical and chemical properties of the measured aerosols.

Our continental aerosol measurements typically showed an aerosol consisting of primary crustal particles with radii $r > 0.5$ μm and sulfate particles with $r < 0.5$ μm. Observed bimodal distributions as shown in Fig. 5 suggest dif-

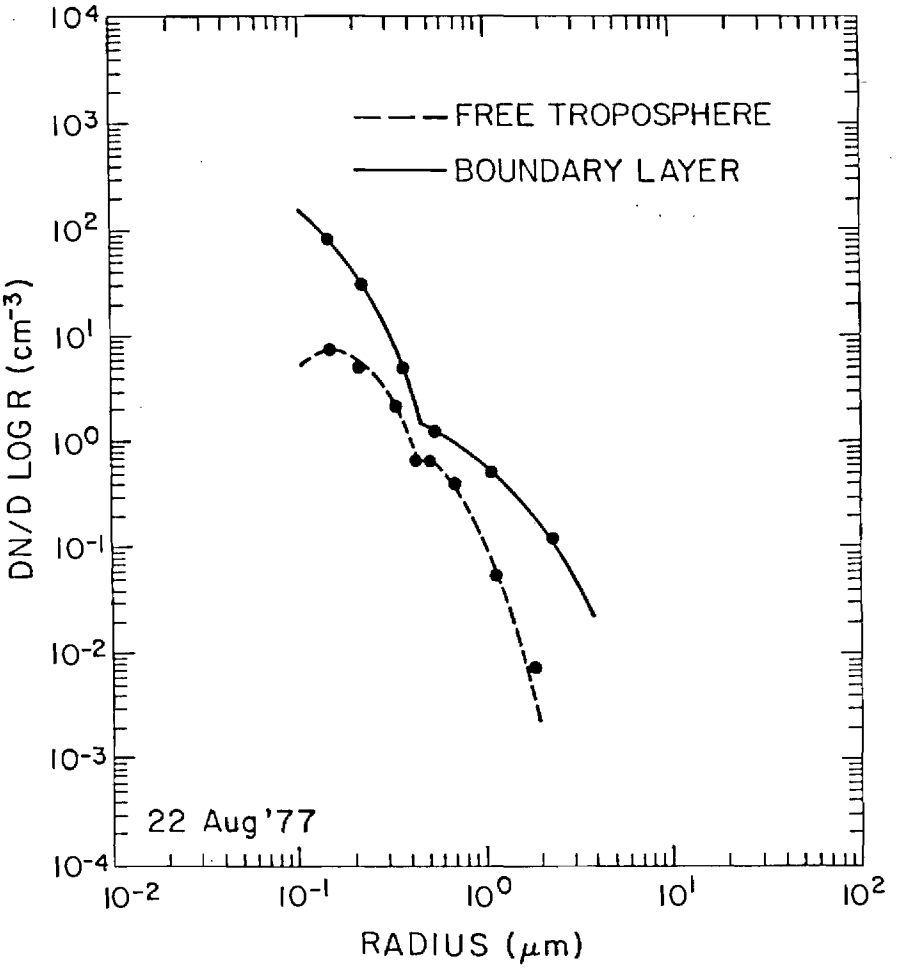

Figure 5

Two typical size-number distributions measured during the GAMETAG program over the southwestern United States. The solid line represents a size distribution measured within the boundary layer and the dashed line represents a free tropospheric distribution. The curves in each case are fits to log normal distributions. Such bimodal size distributions are indicative of multiple source aerosol populations.

ferent aerosol sources for both boundary-layer and free-tropospheric aerosol particles. Our measurements show only a minor sea-salt component in the total continental aerosol population (~4% by mass). While aerosol populations were not qualitatively different from observations made in the continental boundary layer or the free troposphere, a general decrease in total particle number was observed in the free troposphere with the greatest decrease associated with the very largest and the very smallest particles. These similarities in aerosol population are apparently due to mixing between the boundary layer and the free troposphere; the detection of urban trace elements in the free troposphere over California was evidence for this mixing.

Calculations of mass-extinctions ratios for our boundary layer measurements show values ($\sim 4 \times 10^{-3}$ g m^{-3} km) that are intermediate between urban values and rural values in which the extinction is due primarily to soil aerosols. Our data show significant contributions to the total mass loading from primary aerosols in both the boundary layer and the free troposphere suggesting that primary aerosols of crustal origin represent a significant component of the background tropospheric aerosol in western portions of North America and that the contribution of the crustal aerosol to extinction should not be ignored.

In contrast to our continental measurements, Pacific marine measurements such as those shown in Fig. 6 show a qualitative difference between the aerosol population in the marine boundary layer (MBL) and the marine free troposphere (MFT). The Pacific MBL aerosol generally appears to be dominated by sea spray particles with a bimodal distribution that reflects the two major production mechanisms for this aerosol. This sea spray aerosol is present as a hydrated aerosol with radii slightly less than twice the dry radii; the optical effects and total aerosol mass are primarily determined by a large particle mode centered at approximately 1 μm radius on a dV/d log r plot. Elemental analysis indicates that the sea-spray aerosol modes differ in composition, with the small particle mode depleted in Cl relative to S. Our data indicate a loss of particulate Cl in the total aerosol sample due to chemical reactions, with the greatest loss in the smallest particles.

Elemental analysis also shows a minor contribution from a crustal component for the MBL large-particle mode, with the crustal component decreasing

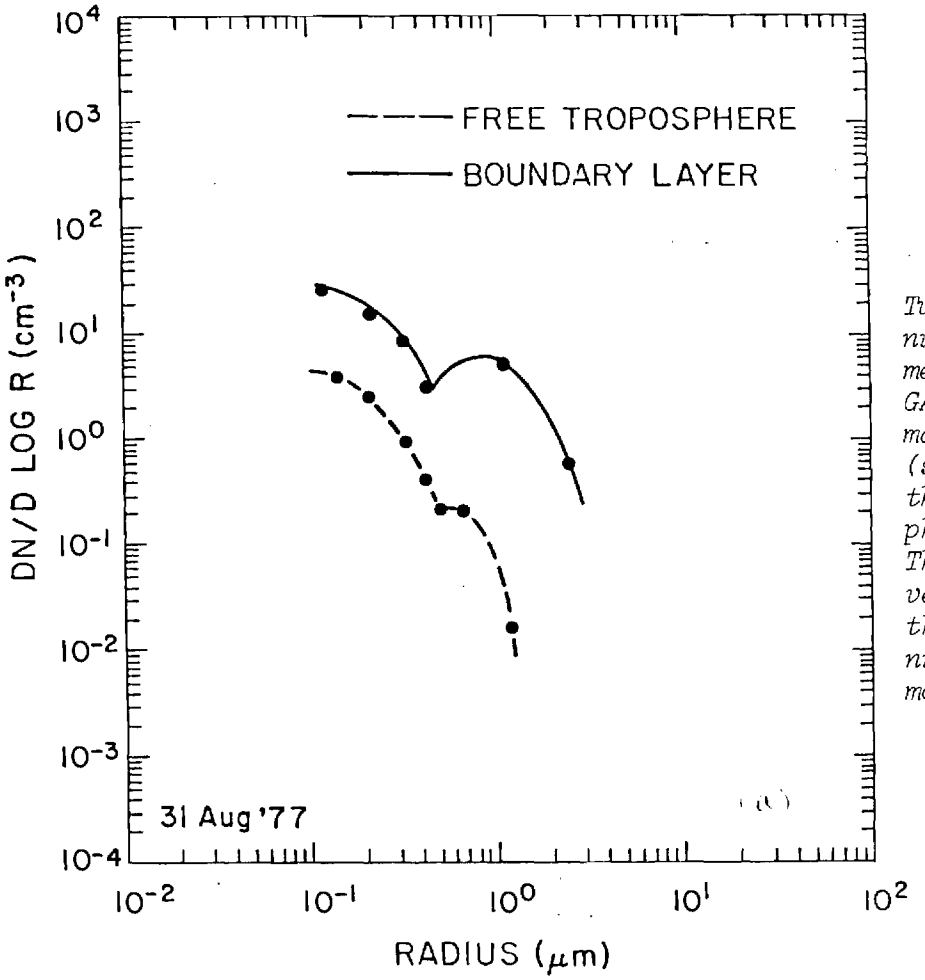

Figure 6

Two typical marine size-number distributions measured during the GAMETAG program for the marine boundary layer (solid line) and for the marine free troposphere (dashed line). The figure shows a very large increase in the total particle number on entering the marine boundary layer.

in concentration from north to south. We observed mean concentrations of 3.8 μg m^{-3} for the dry sea salt component from PMS data and 0.2 μg m^{-3} for the crustal aerosol from Fe concentrations and Mason's (1966) elemental ratios for boundary-layer flights between 40°S and 18°N. Our salt aerosol concentration is lower than the previously reported mean due to the lower salt aerosol concentrations at our MBL flight altitudes (∿300 m) than at the surface.

We have used PMS data on the variations in the large and the small particle modes to infer an average background aerosol concentration in the marine boundary layer of 0.22 μg m^{-3} (0.2 ppbm) dry aerosol weight for aerosols with radii greater than 0.15 μm. We identified some of these particles as locally produced secondary aerosols; simultaneous measurements of gas phase chemical species support this conclusion.

Our Pacific free-troposphere measurements show a highly variable aerosol population. The total concentration varies between 2.4 μg m^{-3} and 0.015 μg m^{-3}. Primary crustal aerosols transported from continental areas appear to be a major component of the Pacific free tropospheric aerosol north of 18°N; the concentration of these crustal aerosols shows a general decrease from north to south along our flight tracks across the Pacific. The northern Pacific free tropospheric aerosol population appears to be dominated by transport from continental areas. Sources for the southern hemisphere secondary aerosols have not been determined, but the aerosols in this size range show a marked variability, with changes in concentration by more than an order of magnitude within a few minutes of aircraft flight time.

In Fig. 7, latitude profiles along our flight tracks show higher total

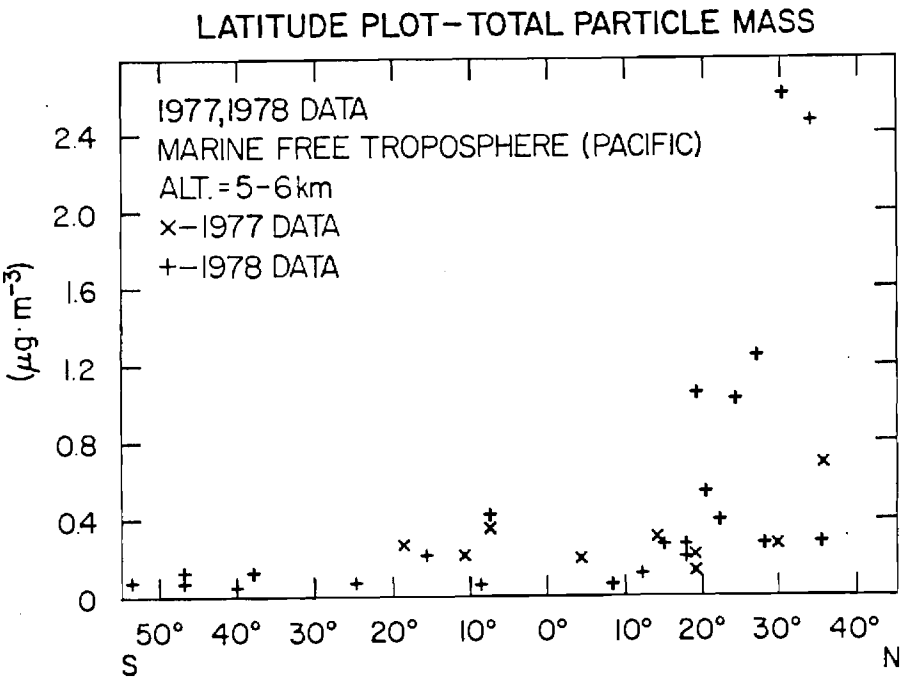

Figure 7

Total particle mass calculated from the PMS data for the marine free troposphere measurements during the GAMETAG program plotted against the latitude along the aircraft flight tracks for the 1977 (x) and the 1978 (+) data.

aerosol concentration in the northern than the southern hemisphere, with lowest concentrations south of 20°S. Our geometric mean concentration for particles with radii greater than 0.15 μm was 0.8 ppbm north of 18°N decreasing

to 0.08 ppbm south of 20°S. We identified this concentration of 0.08 ppbm as a background concentration for the aerosol population at this altitude; this value is significantly less than the inferred MBL background concentration of 0.2 ppbm.

Conclusions

The GAMETAG aerosol measurements were performed to provide a data base for the assessment of the causal relationships between aerosol populations and the factors controlling aerosol populations, to provide an assessment of the levels and types of aerosols in remote regions in both the planetary boundary layer and in the free troposphere, and to provide an initial assessment of the possible impact of tropospheric aerosols in these remote regions on climate and atmospheric visibility. These objectives were successfully accomplished.

Detailed discussions of the GAMETAG aerosol results are provided in the paper attached as an appendix to this report. In addition, data on the optical properties of the aerosols obtained in the GAMETAG program will be used in a continuing program at Georgia Tech to validate and improve models of the radiative effects of aerosol particles. We believe that the results of the GAMETAG aerosol study have demonstrated that simultaneous measurements of the meteorological state variables, related chemical gaseous species, and the chemical physical, and optical properties of the atmosphere aerosol is an effective approach for future work to further our understanding of the behavior and impact of the tropospheric aerosol.

References

Grams, G. W., 1980: In-situ light scattering techniques for determining aerosol size distributions and optical constants. Light-Scattering by Irregularly Shaped Particles (D. W. Scheurman, ed.), Plenum Publishing Corp., pp. 243-246.

Grams, G. W., I. H. Blifford, Jr., D. A. Gillette, and P. B. Russell, 1974: Complex refractive index of airborne soil particles. J. Appl. Meteor., 13, 459-471.

Grams, G. W., A. J. Dascher, and C. M. Wyman, 1975: Laser polar nephelometer for airborne measurements of aerosol optical properties. Optical Engineering, 14, 85-90.

Hansen, J. E., 1969: Exact and approximate solutions for multiple scattering by cloudy and hazy atmospheres. J. Atmos. Sci., 26, 478-487.

Henyey, L. G. and J. L. Greenstein, 1941: Diffuse radiation in the galaxy. Astrophys. J., 93, 70.

Mason, B. J., 1966: Principles of Geochemistry, 3rd edition, Wiley and Sons, New York.

Patterson, E. M., D. A. Gillette, and G. W. Grams, 1976: The relation between visibility and the size-number distribution of airborne soil particles. J. Appl. Meteor., 15, 470-478.

GLOBAL MEASUREMENTS OF AEROSOLS IN REMOTE CONTINENTAL AND MARINE REGIONS: CONCENTRATIONS, SIZE DISTRIBUTIONS, OPTICAL PROPERTIES

by

E. M. Patterson, C. S. Kiang
School of Geophysical Sciences
Georgia Institute of Technology
Atlanta, GA 30332

A. C. Delany, A. F. Wartburg
National Center for Atmospheric Research
Boulder, CO 80307

A.C.D. Leslie
Department of Oceanography
Florida State University
Tallahassee, FL 32306

B. J. Huebert
Department of Chemistry
Colorado College
Colorado Springs, CO 80903

ABSTRACT

The phase I GAMETAG aerosol measurements were designed to provide an initial assessment of the levels, types, and optical effects of tropospheric aerosols in remote marine and continental regions and to examine the possible causal relationships between the observed distributions and the dominant factors controlling aerosol population: chemical and physical transformations, source and sink strengths, and transport. We used size-number data to determine mass concentrations and to estimate extinction, using nominal optical properties. Filter and impactor data have been used to determine aerosol composition, and correlative aircraft measurements have been used to aid in our data interpretation. Our data have been used to generate latitudinal profiles along our Pacific flight tracks.

Our continental measurements, in general, show bimodal aerosol size distributions that reflect different sources for each mode. The aerosol population consists primarily of crustal aerosols with $r \geq 0.5$ μm and sulfate and combustion aerosols with $r < 0.5$ μm, with only a minor sea salt component. Due to vertical mixing, there are no qualitative differences between the boundary layer and the free troposphere. Our data indicate that crustal aerosols represent a significant component of a background tropospheric aerosol in western North America and suggest that the possible contribution of the crustal aerosol to extinction should not be ignored.

Pacific marine measurements show a qualitative difference between the boundary layer and the free troposphere. The boundary layer aerosol population is dominated by a bimodal sea spray aerosol; optical effects and mass concentraion are dominated by a mode with a volume mean radius of ∿1 μm. Our measurements show only a small crustal component of the marine boundary layer aerosol. Our data indicate a loss of Cl from the sea spray aerosol, with the greatest loss in the small particles. We have inferred a background concentration of 0.2 ppbm for our measured particles that does not appear to be directly related to the sea spray aerosol. We have identified some of these particles as locally produced secondary aerosols; simultaneous measurements of gaseous species support this interpretation. Our Pacific free tropospheric aerosol measurements show a highly variable aerosol component, with local variations in concentration by an order of magnitude within a few km. Our measured total aerosol and crustal component concentrations show a general decrease from North to South. Our lowest mean midtropospheric concentration was seen south of 20°S; we have identified this mean concentration of 0.08 ppbm as a midtropospheric background aerosol.

INTRODUCTION

The Global Atmospheric Measurement Experiment of Tropospheric Aerosols and Gases (GAMETAG) has had as its objective the coordinated measurement of those atmospheric trace species (gases and aerosols) that are necessary to gain an understanding of atmospheric chemical properties and processes. In particular the aerosol measurements of the Phase I GAMETAG program were designed to measure the levels and types of tropospheric aerosols, both in the mid or free-troposphere and in the planetary boundary layer, under a variety of remote conditions, to assess the causal relationships between these observed distributions and the dominant factors controlling aerosol populations, and to study the optical effects of the aerosols, as an indication of possible climatic impact.

We are reporting aircraft measurements of aerosol size-number distributions from which we have calculated mass concentrations and optical extinctions. Filter and cascade impactor data have been used to determine aerosol composition as a function of particle size; correlative chemical measurements and meteorological observations have been used as an aid in the interpretation of the size-number-composition measurements.

We have discussed the sources and generation mechanisms for both continental and oceanic areas, as well as the relative importance of individual aerosol types, and the role of transport, transformation, and removal mechanisms in producing the measured aerosol distribution and its variability. We have addressed the question of a background aerosol in the remote areas of the Pacific for both the boundary layer and the mid-troposphere. We have, in addition, presented latitudinal profiles of aerosol concentration and extinction along our aircraft flight tracks for our Pacific measurements.

GAMETAG FLIGHT PROFILES

The GAMETAG flight patterns for the 1977 and 1978 Phase I operations are shown in Fig. 1; representative GAMETAG flight profiles are shown in Fig. 4 and 15. In general, the flights consisted of sampling legs in both the midtropospheric region (5-6 km altitude) of the free-troposphere (that portion of the troposphere not directly influenced by the surface) and in the planetary boundary layer (0-2 km altitude), with sounding data taken on the ascents and descents available to link the measurements in the two regions.

Because of the variability encountered in the aerosol populations, we consider the data obtained on these flights as snapshot pictures of the aerosol during the flights rather than as climatological means or continuous records. The data were taken during two seasons, with most of the flights centered around local noon for maximum photochemical activity. Because of the scientific objectives of the program, the flights were planned to avoid regions of strong convective activity and to avoid cloud penetrations as much as possible. Thus, the measurements emphasize clear air data.

INSTRUMENTATION

Size distributions were measured by two general methods during the Phase I GAMETAG program: light-scattering techniques using single-particle optical counters and microscopic techniques involving electron microscopic analysis of particles collected onto Nuclepore polycarbonate filters.

Two optical particle counters manufactured by Particle Measurements Systems (PMS) of Boulder, Colorado, were used on the NCAR Electra aircraft during GAMETAG. A combination Active Scattering Aerosol Spectrometer and Classical Scattering Spectrometer Probe (ASAS-CSSP) was mounted within the aircraft and sampled air from an aerosol inlet manifold, which also supplied the sample air for the filter samples. The aerosol inlet manifold was designed to sample air isokinetically from the outside of the aircraft, to have a diffuser section to reduce the air speed within the sample tube, and to have a series of intakes for each of the aerosol measurement devices. All intakes were operated approximately isokinetically, and the entire system was wind-tunnel tested for sampling efficiency. Such testing showed sampling efficiencies of 1 for particles with $r \leq 0.75$ μm. Sampling efficiency decreased for the larger particles, and so an externally mounted probe, the Forward Scatter Spectrometer Probe (FSSP) was used to measure the large particles. Although each probe is a multi-range device (for a complete description, see the ASAS and FSSP manuals, available from PMS), only one of the ranges for each probe was used in the analysis of the size data:

0.25 μm $\leq$ r $\leq$ 3.0 μm for the FSSP and 0.15 μm $\leq$ r $\leq$ 0.75 μm for the ASAS. Each of the probes has been extensively calibrated by the manufacturer and by two of the authors (Delany and Wartburg) using polystyrene latex spheres and glass spheres for the particle ranges used. Our determination of sizes from the optical particle counter data is based on the polystyrene and glass sphere calibration, with no explicit use of calculations for the differing response of the instruments to particles with differing refractive indices. Our calculations of the Mie scattering functions appropriate to the PMS optical geometry, as well as those reported by Pinnick and Auvermann (1979), indicate that for the range of sizes and refractive indices encountered in this experiment the differing instrumental response characteristics will have no significant effect on our measured size distributions. Because the Mie response functions exhibit double valuedness, we have combined the PMS size intervals into a smaller number of wider intervals that were actually used in our analysis.

The data from the PMS probes are transferred to the Electra Electronic Data Management System tape every two seconds, but for analysis, these second-by-second averages are converted to longer time averages to reduce statistical fluctuation. Comparisons of the PMS size distributions with polar scattering data indicate that the measured PMS distributions are consistent with that expected for the polar scattering data.

The filter measurement procedures and analytical techniques have been described by Patterson and Gillette (1977). These Scanning Electron Microscopy (SEM) techniques allow a determination of particle size number distributions, as well as a direct visual observation of particle morphological characteristics. The SEM analysis can also provide composition data on a single particle basis with energy dispersive spectroscopy (EDS). The combina-

tion of elemental compositional information and morphology allows the identification of the various aerosol components. Crustal aerosols, for example, are characterized by a definite particle morphology and an elemental composition that includes the elements Al and Si along with Fe, Ca, and Mn in approximate crustal ratios. Our filter measurements provide a complementary data set to that provided the the optical particle counters, making it possible to infer aerosol type and source on a single-particle basis.

A low-volume, Battelle-type, single-orifice, two-stage cascade impactor (Mitchell and Pilcher, 1959) collected size separated particle samples for elemental analysis using proton-induced X-ray emission spectroscopy (PIXE) as described by Johansson, et al. (1975). As operated, the impactor consisted of a single impactor stage and a backup 0.4 μm Nuclepore filter. The 50% cut-point for the impactor stage was at approximately 0.75 μm aerodynamic radius. With an expected particle density between 1.0 and 2.0 g cm^{-3}, this corresponds to an actual radius of ∿0.5 μm. The PIXE analysis was performed on the Florida State University tandem Van de Graaff accelerator using procedures described by Lawson (1978) and Darzi (1978).

The efficiencies of these Nuclepore filters for the smaller size aerosols have been investigated by Spurney, et al. (1967) and by Liu and Lee (1976). Based on these studies and on data presented by Cahill, et al. (1977, 1979), we expect that the 0.4 μm filters used in this study will be approximately 100% efficient for the particle with $r > 0.5$ μm and will have efficiencies greater than 80% for all smaller sizes.

We have also used data on the concentration of particulate ionic species (described by Huebert and Lazarus-JGR, this issue) to interpret our optical particle counter data. These ionic concentrations were determined using samples

collected with a high volume sampler aboard the Electra; concentrations of particulate Cl^-, SO_4^{--}, NO_3^{--} and NH_4^+, as well as gaseous HCl and HNO_3 were determined using standard laboratory chemical techniques. These determinations were based on total particulate samples rather than size separated samples, as in the case of the elemental measurements.

DATA PRESENTATION

The size-number distribution data has been converted to dN/d log r and dV/d log r formats (Junge, 1963), with particle concentrations referenced to ambient volume elements measured with laminar-flow volume-flow meters. As discussed earlier, our data have been grouped into two general sets, mid-tropospheric and boundary layer, for both continental and marine samples. The data may be integrated over the period of a leg or some shorter time interval over which the aerosol population does not change, or they may be displayed as a time sequence plot. These time-integrated data allow the generation of an equivalent aerosol "sample" for comparison with filter samples or for internal data comparison; the time sequences provide a graphic display of the variation in aerosol parameters as a sampling flight progresses. The basic particle size-number data may be displayed, or moment calculations for other quantities of interest may be made. In this report, we have calculated aerosol volume, mass, and extinction, with the total mass calculated assuming an appropriate density. In general, we assumed a ρ of 2 g cm^{-3}, although in specific cases (the marine boundary layer, for example) other estimates were used. Aerosol extinction was determined using Mie theory and appropriate optical parameters as described in Patterson, et al. (1976).

Our measured aerosol populations often exhibited a bimodal structure, with a different particle composition associated with each mode. In our data,

as in a number of other data sets (see Patterson and Gillette, 1977 for discussion), the break point between the modes was at approximately 0.5 μm radius. Consequently, we have considered two aerosol populations in a number of cases: one which we have called large aerosols, those with $r \geq 0.5$ μm (the "giant" particle range of Junge) and one which we have called small aerosols, those with $r < 0.5$ μm (the "large" particles discussed by Junge).

CONTINENTAL AEROSOL MEASUREMENTS

Two aerosol size-number distributions measured in continental air over the southwestern United States during the 1977 GAMETAG flights are shown in Fig. 2. The solid curve shows a continental boundary layer distribution, and the dashed curve shows a size distribution obtained at the nominal mid-tropospheric flight level of 5.5 km.

The free-tropospheric size distribution shows a decrease in particle counts for all sizes relative to the boundary layer size distribution, with a relatively larger decrease for the largest and the smallest particles. This behavior, a general feature of our measurements, is consistent with the preferential removal of the larger particles by sedimentation and of the smaller particles by coagulation discussed by Blifford and Ringer (1969).

Each of these distributions is bimodal, indicating the importance of more than one source for the aerosol population. Similar bimodal continental boundary layer aerosol distributions have been reported by a number of investigators (Whitby, et al., 1972; Wiellike, et al., 1974; Sverdrup, et al., 1975; Patterson and Gillette, 1977a). We are not aware of similar measurements and interpretation in terms of a multimodal structure for free-tropospheric aerosol populations, although qualitatively similar size-number distributions for comparable free-tropospheric altitudes were reported by Blifford and

Ringer (1969).

The composition of these aerosol populations was determined by a combination of chemical and microscopic techniques; these analyses showed two distinct aerosol populations. Those particles with $r > 0.5$ μm (our larger particles) were generally crustal aerosol particles. The identification of these crustal particles was made on the basis of morphology and elemental composition of individual particles and on the elemental composition determined by the PIXE analysis. The PIXE analysis showed that these large particle samples contained the crustal suite of elements in both the boundary layer and the free-troposphere; enrichment factors calculated for these elements (Rahn, et al., 1977) are near unity in both the boundary layer and the free-troposphere, as shown in Table 1, confirming a crustal source for these particles. The possible importance of a sea salt aerosol component in this large particle mode of the continental aerosol was estimated by analyzing the Cl/Fe ratios determined by PIXE analysis, using Cl as a marker for the sea salt component and Fe as a marker for the crustal component. The use of Cl as a marker element has uncertainties due to the reactive nature of Cl and the possibility of non-marine sources for the element (see further discussion of these points below); but, if we assume that all of the Cl in the sample is due to sea salt and that the Cl losses may be neglected, and if we assume that the Fe is present in normal crustal ratios (5% estimated by Mason, 1966), the calculations give a maximum sea salt concentration of approximately 4% of the crustal aerosol concentration for each of the samples. These results are in general agreement with similar data reported by Delany, et al. (1973) for continental and marine samples.

SEM analysis of the smaller particles by comparison shows them to be

amorphous sulfur containing particles of a size consistent with that expected for secondary particles. In addition, the measured small particle concentrations are consistent with the measured concentrations of sulfate, nitrate, and ammonium ions-ionic species associated with secondary aerosol populations.

This consistency was demonstrated by calculating the total mass concentration associated with the measured ionic species and comparing this mass concentration with that inferred from the PMS small particle mode, assuming a specific gravity of 2. These calculations were performed for two samples, a boundary layer sample over the Imperial Valley of California and a free-tropospheric sample taken between California and Colorado.

Based on the observed free-tropospheric size distributions (see Fig. 2), no significant fraction of the mass is associated with particles smaller than those measured with the PMS probes. Our boundary layer measurements do, however, suggest that a significant portion of the total aerosol mass will be associated with these particles with $r < 0.15$ in.--as expected near sources for secondary and combustion aerosol particles. Data of Wiellike, et al. (1974) near aerosol sources, and analytic fits to our Imperial Valley boundary layer sample suggest that 25 to 50% of the small particles mode mass will be associated with these $r < 0.15$ μm particles. For the free-tropospheric sample the PMS data gave a concentration of $0.75 \pm .25$ ppbm while the chemical data gave a concentration of 0.5 ± 0.1 ppbm; the Imperial Valley boundary layer sample had a mass inferred from the chemical concentration data of 2.8 ± 0.2 ppbm while the mass inferred from the PMS probe was 3.3 ± 1.5 ppbm. The calculated mass concentrations are consistent within the experimental uncertainties, suggesting that the small particle mode does consist primarily of the measured ionic species such as SO_4^{--} and NO_3^{--}.

The aerosol population does, however, include a component due to direct

production by combustion processes. The free-tropospheric sample contained significant amounts of Ni, Pb, and Br, suggesting the presence of automative exhaust products, an indication of the mixing of urban air containing primary combustion products into the free-troposphere over California. We have not measured organic species, and our data are not able to exclude the possibly significant contribution of organic aerosol components.

Although detailed calculations were done for only these two samples, SEM analysis of our other continental aerosol samples showed similar aerosol characteristics: crustal aerosol particles make up the large particle mode while the small particle mode is made up of particles that are morphologically similar to those seen over the southwestern U.S.

The total measured concentration showed a great deal of variability, however. For the two southwestern U.S. samples considered above, the large particle mass concentrations inferred from the PMS data were 4.3 ppbm for the boundary layer sample and 1.2 ppbm for the free-tropospheric sample, giving total concentrations of 7.6 ppbm for the boundary layer sample and 2.0 ppbm for the free-tropospheric sample. By comparison, a 1977 boundary layer sample over the taiga region of northern Canada, while also bimodal, shows much lower concentrations--0.5 ppbm for the small particle mode and 0.3 ppbm for the large particle mode. Our data for the flight legs over northern Canada exhibit much lower aerosol concentration than do our U.S. samples and appear to be more representative of a continental background aerosol.

A qualitative description of the vertical variation of our continental aerosol concentrations between the boundary layer and the free-troposphere may be given with reference to Fig. 3 which is a plot of large and small particle aerosol concentration, temperature, and dew point versus altitude.

The data were taken during a descent over Arizona, but are representative of our data over western North America.

The temperature and dew point data show a somewhat ill defined boundary layer. The sounding shows a region of slightly enhanced stability below 3 km. As the aircraft descended below this altitude, there was a noticeable increase in the turbulence, suggesting that the well mixed region extending to the surface (the continental boundary layer) extends to an altitude between 2 and 3 km. The dew point curve suggests possible other layers at $\sim$3.5 and 4.8 km. In general, the sounding suggests a reasonably uniform atmosphere extending at $\sim$5 km.

The aerosol counts decrease relatively slowly with increasing altitude. Since our flights were made during times in which surface heating and convective activity over these arid surfaces were important, we infer that convective activity in the region has caused vertical mixing of both the large and the small aerosol from the boundary layer into the free-troposphere. For this location, the mixing appears to be most effective up to a height of $\sim$4 km. Similar midlatitude tropospheric data of Delany, et al. (1973) representing average behavior over a period of more than one year show a similar behavior with most of the aerosol mass below 3-4 km.

Because of this mixing, we would not expect great differences in composition between the free-tropospheric and the boundary layer aerosols under our measurement conditions; and no great differences were seen in particle morphology, in the shapes of aerosol size distributions, or in the calculated enrichment factors. The differences between the boundary layer aerosol population appear to be more quantitative than qualitative. The variation seen in our continental GAMETAG measurements and in other measurements may be inter-

preted in terms of differing relative importance of aerosol sources and the importance of transport and transformation processes. Our Imperial Valley boundary layer sample for example was taken close to sources for both primary and secondary particles, and so there are higher than background concentrations and significant mass associated with particles in the transient nuclei range. As the aerosols age and are transported from their sources, both the largest and the smallest particles will be removed by sedimentation and coagulation, and there will be a general decrease in concentration. This is seen both in our free-tropospheric samples and in our more remote boundary layer samples.

An example of the variability seen in our aerosol measurements is shown in a set of time sequence plots (Figs. 4a-d) for the flight path from Denver to San Francisco in the 1977 flight series. The mass and extinction are calculated from the PMS data; the fluctuations in the values determined for the larger particles are partially due to the small number of particles measured. The extinction calculations assumed a refractive index of 1.5-.005i, a value based on previous measurements by Grams, et al. (1974). The greatest uncertainty in the refractive index estimate is the value for the imaginary index, but previous calculations have shown that the calculated extinction will not be strongly dependent on the value of the imaginary index of refraction, particularly for the larger particles (Patterson, et al., 1976) so the value calculated should be representative of the true aerosol extinction.

For this flight, the total mass concentration varied by roughly three orders of magnitude, the relative contributions from the large and the small particles varied by much smaller amounts, however. This sequence shows slightly more mass in the small mode above the boundary layer, but within the boundary

layer the mass was dominated by the large particles.

The extinction calculations showed roughly equivalent contribution to the total particle extinction from each mode, both above and below the boundary layer, with a calculated total extinction below the boundary layer of roughly 2×10^{-8} cm^{-1} in the relatively unpopulated areas of Arizona, increasing to more than 3×10^{-7} cm^{-1} in the more densely populated and farmed areas between Yuma and the Imperial Valley. Even when passing through the high aerosol concentrations near Yuma (approximately 21:30) and the Imperial Valley (between 21:50 and 21:10), the increase in primary and secondary particles was such that the relative contribution of each to the extinction remained about the same. Calculations of the mass-visibility constant using the notation described in Patterson and Gillette (1977b) results in a value for C of approximately 4×10^{-3} $g\ m^{-3}$ km, a value roughly two times the values measured for urban aerosols (Charlson, 1969), but considerably less than the values for soil-derived aerosols only.

This time sequence and the sample data sets discussed above are consistent in suggesting that under background or near bakcground conditions in rural, western North America the crustal aerosol will be a significant part of the total aerosol population. In our measurements, the crustal aerosol is a significant contribution to total extinction and to reduced visibilities.

We certainly cannot claim that the atmospheric conditions of our flights represent mean conditions, but these measurements point up the fact that any control strategy or monitoring strategy designed to maintain desired high-visibility conditions in this region of the arid southwestern United States cannot ignore reductions in visibility due to primary crustal aerosols.

MARINE AEROSOL MEASUREMENTS

Our marine measurements differ from our continental measurements in two significant ways. All of the continental measurements described here were made under conditions of relatively low humidity so that the aerosol was probably present in a dry form. Although our marine free-tropospheric (MFT) measurements were generally made with relative humidities of less than 50%, our marine boundary layer (MBL) measurements were made under conditions of high relative humidity so that the aerosol was present as a hydrated aerosol. Secondly, there were no general qualitative differences between the free-tropospheric and the boundary layer aerosols in our continental measurements; for our measurements in remote areas of the Pacific Ocean, the differences between the MFT and MBL measurements were qualitative as well as quantitative.

Two aerosol distributions measured in a marine environment above and within the boundary layer are shown as size-number distributions in Fig. 5a and as volume-number distributions in Fig. 5b. The solid line represents an MBL aerosol distribution while the dashed line is an MFT distribution--in this case above a trade-wind inversion. There is an even more dramatic increase in particle volume within the boundary layer than in the continental cases, and each of the two MBL modes have larger mean radii, reflecting the fact that the MBL aerosol is a hydrated aerosol. The bimodality is, as discussed below, a general feature of the MBL aerosol population; a bimodal structure for the free-tropospheric aerosols is not always clearly seen, particularly in the southern hemisphere Pacific measurements.

A representative sounding plot for our marine data is shown in Fig. 6. This sounding shows a gradual decrease in particle counts in both the large and small particle ranges with increasing altitude within the boundary layer,

a rapid falloff in counts at the top of the boundary layer, and relatively uniform counts in the free-troposphere. The sounding is consistent with local generation of aerosols at the ocean surface, turbulent transfer within the well mixed MBL, and little direct mixing between the MBL and the free-troposphere under the stable conditions shown here. In general, as in this specific case, the trade wind inversion or other areas of enhanced stability in tropical or subtropical regions can provide a strong cap for the boundary layer aerosols; in these regions, the MFT aerosol population will be strongly influenced by horizontal transport.

Since the data indicate a sea surface source for the aerosols, the aerosol concentration should be related to the sea state. A useful parameterization, then, for aerosol concentration is wind force, measured on the Beaufort scale. Three GAMETAG MBL size-volume distributions parameterized according to the Beaufort scale are shown as the solid lines in Fig. 7. The wind force was estimated from wind speed measurements at the flight level of the aircraft, corrected to an assumed wind speed at the standard height of 11 m above the surface using a logarithmic wind profile in the boundary layer and a surface roughness of 0.001 m. The net effect of the correction was a reduction in wind speed to a value approximately 70% of the value at our flight altitudes of 250-500 m.

The bimodality of the distribution is clearly seen in each case, as is the increase in total particulate loading with increasing wind force. Even in cases where there is not a clearly defined peak, there is certainly more aerosol volume in the size range $r < 0.5$ μm than would be expected on the basis of a unimodal distribution. These size distributions are similar to MBL size distribution curves presented by Woodcock (1972) and Meszaros and

Vissy (1974), as well as bimodal elemental distributions of Meinert and Winchester (1977). There are, however, some significant differences between our measured size distributions and those measured by Woodcock (1953) and presented as volume distributions by Junge (1963)· the Woodcock size distributions have larger volume mean radii than do ours, with a greater increase in mean radius with increasing wind force. The difference in mean radius is seen in Fig. 7 in which the dashed line represents one of Woodcock's distributions appropriate to a wind of Beaufort force 5.

Woodcock's data are clearly different from ours; consideration of possible reasons for the differences suggest differing measurement techniques as well as differing environmental conditions. Woodcock's data are based on impaction of aerosols onto collection substrates followed by counting of rehydrated samples, while ours are in situ optical particle counter data. Possible errors in particle sizing using impaction techniques for stratospheric aerosols have been discussed by Farlow, et al. (1979); their results suggest a downward correction in measured size for larger aerosols. With regard to different conditions of sampling, Woodcock's measurements were apparently made under conditions of more convective activity than were ours. Our measurements were made under reasonably stable conditions, and our profiles suggest that there is a more rapid decrease in particle concentration with altitude for the larger particles than for the smaller particles within the MBL (see Fig. 6). Size distributions measured near the surface, then, could have larger mean sizes than do our size distributions; and strong convective mixing could lead to differences in average size measured at aircraft altitudes.

Since the MBL aerosol populations are present as hydrated aerosols,

particle volumes calculated from the optical particle data will include a salt component, water, and possibly other components. To fully interpret our PMS data, we need to calculate a dry aerosol mass; this may be done using experimental data on particle growth. As a check on the overall consistency of the total aerosol data set, in view of the discrepancy between our data and Woodcock's data, we have compared the dry aerosol component inferred from the large particle mode of PMS data with that inferred from the Cl^- measurements of Huebert (JGR, this issue) for the 1978 data set.

The optical particle counter volume distributions were converted to dry aerosol mass concentrations using data (from Winkler, 1973, and Winkler and Junge, 1972) on the increase in radius of sea salt particles with increasing relative humidity, data which does not differ significantly from data of Junge (1963), Hanel (1976), Woodcock (1953), or Winkler (1977). Our humidities in the tropical and subtropical marine boundary layers ranged between 75 and 87% with no obvious dependence of size distribution on humidity. With an assumed average relative humidity of 80%, we would expect an increase in particle radius of slightly less than a factor of two: for our conversion, we assumed an increase in volume such that the resulting hydrated aerosol volume is six times the dry aerosol volume. This volume increase corresponds to m_w/m_o ratio (ratio of water mass to dry aerosol mass) of 2.4 assuming a specific gravity of 2.1 for the dry sea salt aerosol.

The Cl^- data were first corrected for errors introduced due to the subisokinetic sampling, making use of the optical particle counter size distributions. The corrections were made as described in Patterson and Gillette (1977a). Assuming that the Cl^- mass distribution is given by the large particle volume distribution, the corrections resulted in lowering

of the measured MBL Cl^- mass concentration by a factor of 2.1. The adjusted Cl^- data were then converted to a total sea salt aerosol concentration by multiplication of the Cl^- data by 1.8, the ratio of total salt mass to Cl^- mass in sea water, assuming no Cl loss in the aerosol, an assumption discussed further below. The comparison is shown in Fig. 8, with the data plotted in units of $\mu g\ m^{-3}$. The regression equation of the dry salt component determined from the PMS data versus the dry salt component determined from the chemical data with the line constrained to pass through 0 is NaCl (PMS) = 1.29 NaCl (Chem), indicating a reasonable agreement between the two data sets.

To further compare our data with previous data sets, we have plotted the dry aerosol mass inferred from the PMS data against wind force for each of our samples. These data are shown in Fig. 9, which we have adapted from Junge (1963). Our data appear to be consistent with the previous data of Woodcock (1953), Junge (1954), and Moore (1952). The 1977 data show generally higher mass concentrations for a given wind force than do the 1978 data, which we attribute to differences in the meteorological conditions for the two years.

Since Fig. 7 suggests that the particle volume in the two MBL modes is related, we have sought to quantify that relationship by determining the best fit line relating the small particle mode volume and the large particle volume mode. This data is shown in Fig. 10; the regression equation relating the volume in the two modes is $V_S = 0.29 + 0.028\ V_L$, with V_S being the small particle mode volume and V_L the large particle mode volume, both with units of $\mu m^3/cm^3$. Correlation between V_L and V_S is 0.88.

We interpret these results in a straightforward manner to mean that the small particle mode is composed of two components: one that varies with

the large particle mode having a volume approximately 3% of the large particle mode volume and one that is independent of the large particle mode having a roughly constant volume of approximately 0.29 $\mu m^3\ cm^{-3}$. It seems clear that the large particles consist of sea salt (Meszaros and Vissy, 1974), and so that portion of the small particle mode that varies with the large particle mode may be assumed to have a common, or at least a related, origin. That is, the variable small particle component appears to be due to a primary production mechanism, rather than the secondary production mechanisms responsible for many of the continental aerosols in this size range.

Although both modes have primary production mechanisms, there appear to be different production mechanisms for each mode and a different composition for each mode (Winchester and Duce, 1975; Meszaros and Vissy, 1974; Meinart and Winchester, 1977), with the large particles produced by the bubble jet action and the smaller particles by the breaking up of bubble film caps.

Our PIXE analysis of the MBL cascade impactor samples shows differences in aerosol composition between the two modes similar to that previously observed (Meinart and Winchester, 1977). Although our samples were lightly loaded, we were able to determine Cl/S ratios for the MBL sample with the largest Cl loading. For this sample, the Cl/S elemental ratio was 7.9, approximately that measured by Berg (1976) for aerosols produced in the laboratory from an artificial sea water. The small particle mode Cl/S ratio was much lower, $\sim$0.4, compared with a value of $\sim$1 measured by Berg for comparable particles, suggesting that the small particle mode is enhanced in S relative to Cl compared with the large particle mode or with bulk sea water. Previous data (Gravenhorst, 1978) suggest little or no fraction-

ation of the sulfate relative to solium in the generation of sea spray aerosols, and so the observed PIXE Cl/S ratios, ~1/2 that of bulk sea water, support the idea that particulate Cl is lost in the generation process for the aerosol, with the greatest loss occurring in the small particle fraction.

Further support for the idea of Cl loss is given by a comparison of our measured Cl concentrations with Cl concentrations inferred from our measured Ca concentrations (after correction to take account of the crustal contribution to our measured Ca). Previous work (Hoffman and Duce, 1972; Hoffman, et al., 1974) has shown that there is no fractionation between Ca and Na in the sea spray aerosol generation, and so multiplication of the Ca concentrations by the Cl/Ca ratio is sea water provides Cl concentrations assuming no losses of Cl. The comparison is shown in Fig. 11; it is apparent that the inferred Cl concentrations are higher than the measured Cl concentrations, indicating that Cl is lost from the aerosol.

Such chlorine loss has also been observed by Martens (1974) in regions where significant anthropogenic contribution to the aerosol exists and by Darzi and Winchester (unpublished results) over the more remote Indian Ocean where such Cl loss was only detected on the smallest size fraction.

The chemical measurements of Huebert and Lazrus reported in this issue and shown in Fig. 12 show Cl^-/SO^4 ratios consistent with the bulk sea water value. It should be noted that this does not necessarily contradict the PIXE data because of the subisokinetic sampling employed to collect the samples for chemical analysis. Based on our calculations, the measured MBL Cl concentrations appear to be roughly two times too high; the characteristic size of the sulfate particles is smaller than that of the chloride particles, and so there is smaller correction needed to account for errors due to subiso-

kinetic sampling. These considerations suggest a Cl^-/SO_4^{--} ratio somewhat smaller than for bulk sea water, consistent with a loss of chlorine from the aerosol seen in these measurements.

That portion of the MBL small particle mode aerosol population that is independent of the large particle mode may be interpreted as a background aerosol, i.e., one that is present even when there is no primary sea spray aerosol present. So defined, the background will, in general, be less than the average aerosol loading.

From our fitted equation, the background level for the aerosol is estimated to be 0.29 μm^3 cm^{-3}. The GAMETAG data of Huebert show that in the absence of primary aerosol the species SO_4 and NO_3^- are present and dominate the ionic aerosol mass in the MBL. We may then reasonably identify the background as a sulfate aerosol, probably ammonium sulfate (Meszarus and Vissy, 1974). If we assume that the aerosol is a hydrated ammonium sulfate aerosol, the volume of this hydrated aerosol relative to that of the dry aerosol may be estimated from growth data of Winkler and Junge for ammonium sulfate particles. Assuming a relative humidity of 80%, these data suggest an r/r_0 (ratio of hydrated radius r to the dry radius r_0) value of 1.5; similar data of Ahlberg, et al. (1978) suggest an r/r_0 value of 1.3. If we take the average of the two values, 1.4, assuming ρ = 2 g cm^{-3} for the dry aerosol, the hydrated volume corresponds to a dry aerosol mass of 0.22 μg m^{-3}, or 0.2 ppbm. We emphasize that this is a background level for aerosols with hydrated radii in the range of $0.15 \leq r \leq 0.5$ μm or dry radii in the range $0.11 \leq r \leq 0.36$ μm with the lower limit determined by the PMS probes.

Insight into production mechanisms for these sub-micron background aerosols may be gained by a consideration of a particular case, an MBL measure-

ment at 1°S on May 3, 1978. For this MBL data, there was a very low concentration of spray aerosol; at the same time, there was a relatively high measured SO_4^{--} concentration. This situation is illustrated in Fig. 12 which we have adapted from Huebert (JGR, this issue). The circled point, for the 1°S location, has a SO_4^{--}/Cl^- ratio significantly higher than the average for the tropical and subtropical Pacific MBL measurements.

There is consistency between the dry component of the aerosol mass inferred from the Cl^- data and from the PMS data (0.34 $\mu g\ m^{-3}$ for the Cl^- data and 0.51 $\mu g\ m^{-3}$ for the PMS data), but the small particle mode mass inferred from the PMS data is too low to account for the measured SO_4^{--} concentration. The PMS dV/d log r distribution shown in Fig. 13 , however, unlike the higher Beaufort force concentrations in Fig. 7 , shows an increasing particle volume with decreasing size for the smallest particles, implying that a significant portion of the particulate volume is in a size range smaller than that measured by the PMS probe. We have used the measured sulfate concentrations to extend the PMS volume distributions to smaller size ranges.

For this sample, the primary sulfate associated with the spray aerosol production, determined from the Cl^- concentration, is approximately 0.02 ppbm, compared with a measured SO_4^{--} concentration of approximately 0.40 ppbm. We assume that all of the remaining sulfate is associated with the small particle mode. The volume of this aerosol is calculated by assuming that the aerosol mass is composed only of the sulfate ion (neglecting the mass contribution of any other ionic species) and that the hydrated aerosol has a volume 2.8 times that of the dry aerosol. The aerosol volume determined from the PMS data (0.21 $\mu m^3\ cm^{-1}$) is subtracted from the volume inferred from the SO_4^{--} data (1.2 $\mu m^3\ cm^{-3}$) and the remaining volume is inferred to be associated with

particles smaller than 0.15 μm radius. On the basis of continental measurements, it is expected that all of the significant mass will be associated with particles with $r > 0.01$ μm; these end points may be used to calculate the dV/d log r value shown in Fig. 13 This inferred volume is consistent with the measured PMS volume distribution, with a large portion of the small mode mass in the size range that is associated with condensation mode aerosols in continental measurements. Times for removal of these condensation mode particles are short; so that long range transport is not likely, suggesting that localized generation of aerosols is taking place. The sizes are those expected from secondary aerosol generation processes and are smaller than the small mode primary particles. Furthermore, the concurrent measurements of gaseous species found that the ozone concentration had reached the lowest level seen during the entire GAMETAG field operation (3 ppb or less), and the SO_2 level was lower than the detection limit. These measurements coupled with the extremely calm meteorological conditions observed during the flight, led us to believe that the low level of O_3 was possibly caused by the photochemical gas phase destruction and that the undetectable SO_2 level was affected by gas-to-particle conversion. These observations, then, strongly suggested that these locally generated aerosols are secondary aerosols.

MFT MEASUREMENTS

Although the MBL measurements may be simply characterized by variation in source input, the marine free-tropospheric measurements show a great deal more variation that reflects the different influences of long-range transport, transport across the boundary layer, and various removal mechanisms.

Transport from continental areas, for example, is significant in the Pacific regions north of the equator. Our MFT data for the Pacific region north of 20° shows mass loadings ranging between 0.2 and 2.4 μg m^{-3}. Bimodal distributions were observed in this region, with the small particle mass approximately equaling the measured SO_4^{--}, NO_3^-, and NH_4^+. SEM analysis showed that these small particles had a morphological and elemental character similar to that of the sulfate aerosol seen in our continental measurements, while the large particles were identified as a crustal aerosol on the basis of morphology and elemental composition (see Table I). The correlation coefficient calculated between V_L and V_S for the Pacific north of 20° is 0.96 (for 10 samples). The particle composition and the correlation between V_L and V_S suggest a continental source for these aerosols, presumably western areas of the United States, with little influence from the marine boundary layer. Confirming the minor influence of the marine aerosol in this region of the MFT, Cl/Fe ratios for the 1978 flight between San Francisco and Hilo suggest that a maximum of approximately 2% of the aerosol mass may be attributed to sea salt aerosol, neglecting possible Cl loss--a value comparable to our continental values.

In more southerly areas of the Pacific, the relative importance of the marine component is greater, due to the decreased importance of transport from continental areas. Our PIXE Cl data suggest that there is a significant marine component of the MFT aerosol along our flight tracks south of Hawaii. As we have discussed earlier, convective activity appears to be the most likely mechanism for injection of this marine aerosol into the free troposphere. Our time averaged filter samples do not show the concentration variations that might be expected from such convective activity. Our PMS data, however, do

show a striking variability in particle size distributions that may be related to convective activity. An example of this variability in the marine midtropospheric size distribution is shown in Fig. 14, which shows data from a 1978 flight at ∿8°S. The two distributions are separated by ∿100 km, but there is a difference of a factor of nearly 100 in the smallest size particles measured. Such changes in the particle size distributions can take place quickly, over distances of tens of kilometers. Such variations in the size distribution were seen in the 1977 series of flights and again in the 1978 series. Special care was taken in the 1978 flights to rule out the possibility of sample contamination; no such possible contamination sources were detected.

We have not identified a source for these anomalously high particle counts; however, similar enhanced particle counts in this size range for measurements made on Mauna Loa above the trade wind inversion in Hawaii were reported by Hogan (1975) who attributed his observations to cloud processes.

Some examples of this variability are illustrated in Fig. 15a-d which show a time sequence plot of a southern hemisphere flight during the 1977 GAMETAG program in the vicinity of Pago Pago, American Samoa. There is an example of a region of anomalously high counts at approximately 21:50, with a corresponding increase in the extinction and mass loading (mass loading increases from ∿0.1 $\mu g\ m^{-3}$ to ∿5 $\mu g/m^3$). There is no increase seen in the larger particle counts in this figure or in Fig. 12; the increase occurs only for the small particles. On the flight sequence shown in this figure, the midtropospheric extinction appears to be dominated by the smaller particles, although there appear to be roughly equivalent mass concentrations in the two size ranges in normal aerosol concentration periods, while the smaller particles dominate both the extinction and the mass whenever these are the

anomalously high counts in the small size range.

LATITUDINAL AEROSOL DISTRIBUTIONS

A plot of the calculated aerosol volume concentration for the hydrated marine boundary layer aerosol as a function of latitude along the aircraft flight track is shown in Fig. 16. If mass concentrations are calculated from the volume concentrations as described above, the dry mass concentrations may be used to determine a geometric mean (GM) and an arithmetic mean (AM) for the sea salt aerosol. We have determined a GM (AM) of 5.9 (7.3) $\mu g\ m^{-3}$ for the northern hemisphere measurements and 2.4 (4.0) $\mu g\ m^{-3}$ for the southern hemisphere, with an overall mean of 3.8 (5.6) $\mu g\ m^{-3}$.

These values may be compared with a GM (AM) of 7.3 (8.4) $\mu g\ m^{-3}$ for sea salt aerosol from ship-based Pacific measurements between 28°N and 40°S reported by Prospero (1979), an AM of 13.0 $\mu g\ m^{-3}$ reported by Hoffman et al. (1977) and Hoffman and Duce (1972) for sea salt measured on Oahu, an AM of 7.2 calculated by Eriksen (1959) for Woodcock's sea salt measurements near Hawaii, and a GM (AM) of 8.4 (9.2) $\mu g\ m^{-3}$ measured by Duce at American Samoa (reported by Prospero, 1979). Our measured boundary layer sea salt concentration may best be compared with the extensive ship based measurements of Prospero. When this is done, we find that our mean values are less than those of Prospero, since sea salt aerosol concentrations decrease with height in the boundary layer.

Our measured MBL Fe concentrations between 12°N and 45°S have a geometric mean value of 10 $ng\ m^{-3}$, with concentrations decreasing from north to south (the GM is 15 $ng\ m^{-3}$ for the northern Pacific data, 7.7 $ng\ m^{-3}$ for the southern Pacific data). Using tabulated relative abundances for crustal elements of Mason (1966), we may infer a value of approximately 0.20 $\mu g\ m^{-3}$

for crustal material.

These values may be compared with a GM of 0.25 $\mu g\ m^{-3}$ for mineral aerosol determined from ship based measurements in the same region by Prospero (1979). Data of Hoffman and Duce for Fe concentration at Oahu show a GM of 9 $ng\ m^{-3}$. Using Mason's value of elemental concentration, we may infer a value of soil aerosol of 0.18 $\mu g\ m^{-3}$. Using a slightly different elemental weighting, Vinogradov (1959), Prospero (1979) calculated a value of 0.24 $\mu g\ m^{-3}$ for the Hoffman and Duce data. Other measurements of Prospero show significantly higher values of mineral aerosol for the region between 26° and 28°N, reflecting transport from continental areas.

The optical extinction may be calculated as a function of dry aerosol mass or total aerosol volume for the aerosol distributions; and the ratio of mass or volume to the extinction may be determined. Such calculations have been described by Patterson and Gillette (1977) and by Pilat and Ensor (1970, 1971). Based on considerations of increase in particle volume under hydrated conditions, and measured values of the index of refraction for sea salt and water, pending analysis of GAMETAG optical properties data, we estimate that the sea salt component of the MBL aerosol in remote regions of the Pacific will have a real index of refraction of 1.37; the imaginary index of refraction will be less than 10^{-4} for wavelengths between 400 and 700 nm. The aerosol consists of liquid droplets, so that Mie theory should apply. Because of the uniformity of the measured size-distributions and aerosol optical properties, a single value of the ratio for volume or mass ratio based on a typical size distribution is appropriate for describing the marine boundary layer aerosol. We have estimated values for these ratios, based on the size distributions and inferred optical properties. The volume-ratio is given by

$$\frac{V}{\sigma_E} = 8.5 \times 10^7$$

where V is the total hydrated aerosol volume in $\mu m^3\ cm^{-3}$ and σ_E is the extinction in cm^{-1}.

The mass-extinction ratio is given by

$$\frac{m}{\sigma_E} = 3 \times 10^7$$

where m is the dry aerosol mass measured in $\mu g\ m^{-3}$ and σ_E in cm^{-1}. Given the relation

$$V_R = \frac{3.9}{\sigma_E}$$

with V_R, the visual range, and σ_E measured in consistent units, these ratios allow us to relate visibility and mass observations and to calculate one from the other.

Similar latitude plots for the midtropospheric total mass concentration and small-particle mass concentration along the aircraft flight tracks are shown in Figs. 17a and b. Both of these figures are based on determinations from the PMS probes including data for both years. Each of these plots are characterized by relatively high aerosol concentrations in the region north of 20°N, between the continental United States and Hawaii. The concentrations are highest in the area closest to the continental United States and decrease to the south and west. The concentrations are different in the two years, reflecting possible differences in transport from continental areas. Total particle mass concentrations are generally lowest in the southern hemisphere, although there can be high total concentrations in the regions of the

anomalously high particle counts. The area south of 20°S was characterized by the lowest average concentration. The arithmetic mean (geometric mean) for our data for this region is 0.065 (0.054) $\mu g\ m^{-3}$ compared with 0.23 (0.18) $\mu g\ m^{-3}$ for the region between 20°S and 18°N and 0.77 (0.51) $\mu g\ m^{-3}$ for the region north of 18°N. The calculated mass concentration in the southern hemispheric MFT is dominated by the particles with $r < 0.5\ \mu m$, while the larger particles (often associated with the crustal aerosol) are more important in our northern hemispheric MFT.

As a confirmation of the increased importance of crustal aerosols in the northern hemisphere, we have plotted the free-tropospheric Fe concentration for the 1978 flight in Fig. 18. It is apparent from the figure that there is a decrease in the Fe concentration from north to south, but our mid-Pacific data suggest that the continental aerosol has a global distribution at this midtropospheric level. If this is the case, then the crustal-derived aerosol is a component of the background aerosol, although our data are not sufficient to determine the relative importance of this aerosol component on a time averaged global basis.

Mass concentrations for crustal aerosols in the northern Pacific obtained using the measured Fe concentration and Mason's crustal abundance data are consistent with the mass concentration inferred from the PMS large particle data. For the remote regions of the southern hemisphere, such comparisons indicate substantially more crustal material than is inferred from the aerosol population with $r > 0.5\ \mu m$ (although less than the inferred total mass). The use of Fe alone to infer a crustal mass in these remote regions is questionable because of the possibility of elemental fractionation in the processes of aerosol generation and transport that leads to enhanced Fe content in the aerosol (Rahn et al., 1977; Rahn, 1976). For example,

elemental concentration data reported by Maenhaut et al. (1979) shows a measured Fe concentration ~8% of their total inferred crustal aerosol. Because of these uncertainties, and the relatively large uncertainties in the measured southern hemispheric MFT elemental concentrations, we have not attempted mass balance calculations to determine the relative concentrations of sulfate and crustal aerosols for this portion of our data sets.

Our data do not allow us to identify the source for these midtropospheric crustal aerosols (southern hemispheric or transport across the equator); other data of Cattell, et al. (1977), who measured elemental Al concentrations at various altitudes up to three kilometers over Tasmania, show a variation in crustal component that suggests a relatively local source, possibly Australia.

Our southernmost Fe data shows a concentration <6 ng m^{-3} (ambient); this may be compared to results of Maenhaut obtained at the South Pole station of approximately 0.6 ng m^{-3}, referenced to STP. The two data sets suggest that there is a continual decrease in concentration of this crustal material toward the Antarctic continent.

Similar MFT PIXE data for Cl along our Pacific flight tracks have a GM of 15 ng m^{-3} for the three southern hemisphere samples, with the same AM; the 0-20°N data have a GM of 0.04 ng m^{-3} and an AM of 0.05 ng m^{-3}. Expressed as mass ratios, the southern hemisphere data have a GM (AM) of 0.02 (0.02) ppbm, while the 0-20°N data have a GM (AM) of 0.06 (0.07) ppbm.

Our lowest mass concentration is 0.015 μg m^{-3} with an AM of 0.065 μg m^{-3} and a GM of .054 μg m^{-3} for regions south of 20°S latitude. For comparison with other measurements these numbers may be converted to mass ratios; expressed in this way, our lowest free tropospheric value is 0.02 ppbm with an AM of 0.09 and a GM of 0.08 ppbm for particles with $r > 0.15$ μm for this

southermost data. We infer that these low southern hemispheric values represent a background level for these midtropospheric aerosols of ∿0.08 ppbm, emphasizing that this background considers only particles with $r > 0.15$ μm. There will often be additional mass loading superimposed on this background level due to transport from continental areas or transport into the midtroposphere from the boundary layer, so that actual values may often be considerably higher than this background level, as we have seen with our tropical and northern data. This suggested midtropospheric background concentration of 0.08 ppbm is less than our inferred marine boundary layer background value of 0.20 ppbm.

The altitude of the South Pole station and the absence of local sources suggest that the South Pole aerosol concentration data should be comparable to our remote midtropospheric data. The mean concentration reported by Maehaut, et al. (1979) was 0.15 ppbm with the lowest measured value equal to 0.11 ppbm with their data effectively averaged by the long sampling times. Our inferred background level appears to be generally consistent with the South Pole data.

The extinction calculated for these midtropospheric aerosols using our measured size distributions and nominal values for the optical properties is shown in Fig. 24. The plot is similar to the plots for midtropospheric mass loading showing a general decrease from north to south. We have calculated an extinction of $\sim 0.2 \times 10^{-8}$ cm^{-1} for latitudes south of 20°S, $\sim 0.7 \times 10^{-8}$ cm^{-1} between 20°S and 18°N, $\sim 2 \times 10^{-8}$ cm^{-1} north of 18°N. Improved estimates of extinction will be reported following analysis of our optical scattering data.

We would like to emphasize again that our results are in the nature of

a snapshot of conditions at two particular times. We cannot say that our data represent climatological means, and we cannot make specific statements regarding long term averages based on our data set alone, except for a few broad generalizations regarding the relative importance of continental aerosols north of 18°N and the low measured concentrations south of 20°S which appear to represent background values for the midtropospheric aerosol. Our data set is consistent with other marine boundary data sets, and our inferences concerning background aerosol levels appear to be consistent with other remote measurements.

CONCLUSIONS

We have used optical particle counter data, elemental and ionic composition information, and particle morphology to obtain a coherent view of the physical and chemical properties of aerosols measured as part of the GAMETAG program.

Our continental aerosol measurements typically show an aerosol population consisting of crustal aerosols with $r > 0.5$ μm and sulfate aerosols with $r < 0.5$ μm. When plotted as a volume distribution, bimodal distributions, reflecting the different aerosol sources, were obtained for both the boundary layer and free-tropospheric aerosols. We estimate that there is only a minor sea salt component of the total continental aerosol population ($\sim$4% by mass). Aerosol populations are not qualitatively different in the continental boundary layer and the free-troposphere, but a general decrease in total particle number with altitude is observed with the very largest and the very smallest particles showing the greatest relative decrease. The similarities in aerosol population are apparently due to mixing between the boundary layer and the free-troposphere; we have seen evidence of this mixing in the presence of

urban trace elements in the free-troposphere over California.

Calculations of mass-extinctions ratios for our boundary layer measurements show values of the ratio ($\sim 4 \times 10^{-3}$ g m^{-3} km) that are intermediate between urban values and rural values in which the extinction is due primarily to soil aerosols; our data show a significant contribution to the total mass loading from the primary aerosols in both the boundary layer and the free-troposphere. These data suggest that the crustal aerosol represents a significant component of the background tropospheric aerosol in western portions of North America and suggest that the contribution of the crustal aerosol to extinction should not be ignored.

In contract to our continental measurements, the Pacific marine measurements show a qualitative difference between the boundary layer and the free-tropospheric aerosol population. The Pacific MBL aerosol is dominated by a sea spray aerosol with a bimodal distribution that reflects the two major production mechanisms for this aerosol. This sea spray aerosol is present as a hydrated aerosol with radii slightly less than two times the dry radii; the optical effects and total aerosol mass are primarily determined by a large particle mode centered at approximately 1 μm radius on a dV/d log r plot. Elemental analysis shows that the sea spray aerosol modes differ in composition with the small particle mode depleted in Cl relative to S. Our data indicate a loss of particulate Cl in the total aerosol sample due to chemical reactions, with the greatest loss in the smallest particle.

Elemental analysis shows a minor contribution from a crustal component for the MBL large particle mode, with the crustal component decreasing in concentration from north to south. We have determined GM concentrations of 3.8 μg m^{-3} for the dry sea salt component (from our PMS data) and 0.2 μg m^{-3}

for the crustal aerosol (from Fe concentrations and Mason's elemental ratios) for our boundary layer flights between 40°S and 18°N. Our GM salt aerosol concentration is lower than previously reported mean concentrations due to the lower salt aerosol concentrations at our MBL flight altitudes (~300 m) than at the surface.

We have used PMS data on the variations in the large and the small particle modes to infer an average background aerosol concentration in the marine boundary layer of 0.22 $\mu g\ m^{-3}$ (0.2 ppbm) dry aerosol weight for aerosols with radii greater than 0.15 μm. We have identified some of these particles as locally produced secondary aerosols; simultaneous measurements of gas phase chemical species support this conclusion.

Our Pacific free troposphere measurements show a highly variable aerosol population, with a total concentration that varies between 2.4 $\mu g\ m^{-3}$ and 0.15 $\mu g\ m^{-3}$. The highest measured concentrations are in the region north and east of Hawaii where the aerosol population is dominated by continental aerosols--crustal and sulfate--that have been transported over the ocean. South of Hawaii, the concentrations decrease, reaching the lowest average concentration south of 20°S. Although sea salt, sulfate, and crustal components have been seen in the MFT at all latitudes, the observed concentrations depend on such variables as long range transport, vertical mixing, and source and sink strengths. In particular, the concentration of the aerosol in the small size range can vary by more than an order of magnitude within a few tens of kilometers.

Our measured geometric mean concentration for particles with $r > 0.15$ μm south of 20°S was 0.08 ppbm. We have identified this lowest average MFT concentration as a background concentration for the aerosol at this altitude,

a value that is significantly less than the inferred MBL background concentration of 0.2 ppbm.

Estimates of aerosol extinction in the marine environment have been made using our measured aerosol size-number distributions and nominal aerosol optical properties. Based on these data, we have calculated averages of aerosol extinction along our Pacific flight tracks for both the MBL and the MFT data. Our MBL data show an average extinction 1×10^{-7} cm^{-1}; our MFT data show an average extinction of $\sim 0.2 \times 10^{-8}$ south of 20°S ranging up to $\sim 2 \times 10^{-8}$ cm^{-1} north of 20°N. More precise and detailed calculations of the aerosol optical effects will be reported following further analysis of the aerosol optical and scattering properties.

Based upon our studies, it is important to point out the future field measurements on aerosols should stress detailed studies of the cause and effect relationships between the spatial and temporal distributions and the dominant controlling factors, such as source and sink strengths, transformation and transport, to understand the variability of the atmospheric aerosols distribution. The simultaneous measurements of meteorological state variables, related chemical gaseous species, and chemical and physical properties of aerosols are the most important criteria to achieve this basic understanding. In addition to the quantities that have been measured by GAMETAG flights, we strongly recommend that the measurements of size distribution be extended to smaller sizes, that size separated chemical composition measurements be made that organic aerosol components be measured and that aerosol flux and flux gradients be measured.

ACKNOWLEDGMENTS

This work was supported in part by the National Science Foundation through Grant ATM7810091 and by the National Aeronautics and Space Administration through Grant NSG-1493. The National Center for Atmospheric Research is sponsored by the National Science Foundation.

REFERENCES

Ahlberg, M.S., A. C. D. Leslie, and J. W. Winchester, The chemical state of particulate sulfur in ambient aerosols determined by PIXE analysis, Nuc. Inst. and Meth., 149, 451-455, 1978.

Berg, W. W., Chlorine chemistry in the marine atmosphere, Ph.D. Thesis, Department of Oceanography, The Florida State University, 1976.

Blifford, I. H. and L. D. Ringer, The size and number distribution of aerosols in the continental troposphere. J. Atmos. Sci., 26, 716-726 1979.

Cahill, T. A., L. L. Ashbaugh, J. B. Barone, R. A. Eldred, P. J. Fenney, R. G. Flocchini, C. Goodart, D. J. Shadoan, and G. W. Wolfe, Analysis of respirable fraction in atmospheric particulates via sequential filtration. J. Air Poll. Cont. Assn., 7, 675-678, 1977.

Cahill, T. A., R. A. Eldred, J. Barone, and L. Ashbaugh, Particulate sampling with stacked filter units, Report No. FHWARD, Federal Highway Administration, Office of Research, Washington, DC, Available from NTIS, 1979.

Cattell, F. C. R., W. D. Scott, and D. DuCross, Chemical composition of aerosol particles greater than 1 μm diameter in the vicinity of Tasmania, J. Geophys. Res., 82, 3457-3472, 1977.

Charlson, R. J., Atmospheric visibility related to aerosol mass concentration, Environ. Sci. Technol., 3, 913-918, 1969.

Darzi, M., Terrestrial influences on the aerosol composition over the western north Atlantic Ocean, M.S. Thesis, Department of Oceanography, The Florida State University, 1977.

Delany, A. C., W. H. Pollock, and J. P. Shedlovsky, Tropospheric aerosol: The relative contribution of marine and continental components, J. Geophys. Res., 78, 6249-6265, 1973.

Dmokhovski, V. I., L. S. Ivlev, and A. Yu Semova, Measurements of aerosols in the atmospheric layer near the ground in Karakum, Tr. Gl. Geofiz. Observ., 276, 109-112, 1972.

Eriksson, E., The yearly circulation of chloride and sulfur in nature: Meteorological, geochemical, and pedological implications. Part I, Tellus, 11, 1959.

Farlow, N. H., G. V. Ferry, H. Y. Lem, and D. M. Hayes, Latitudinal variations of stratospheric aerosols, J. Geophys. Res., 84, 733-744, 1979.

Grams, G. W., I. H. Blifford, Jr., D. A. Gillette, and P. B. Russell, Complex index of refraction of airborne soil particles, J. Appl. Meteorol., 13, 459-471, 1974.

Gravenhorst, G., Maritime sulfate over the North Atlantic, Atmos. Environ., 12, 707-713, 1978.

Hanel, G., The properties of atmospheric aerosol particles as functions of the relative humidity at thermodynamics equilibrium with the surrounding moist air, in Advances in Geophyics, Vol. 19, Academic Press, New York, H.E. Landsberg and J. Van Miegham, ed., 1976.

Hoffman, G. L. and R. A. Duce, Consideration of the chemical fractionation of alkalai and alkaline earth metals in the Hawaiian marine atmosphere, J. Geophys. Res., 77, 5161-5169, 1972.

Hoffman, E. J., G. L. Hoffman, and R. A. Duce, Chemical fractionation of alkalai and alkaline earth metals in atmospheric particulate matter over the North Atlantic, J. Rech. Atmos., 8, 675-685, 1974.

Hoffman, E. J., G. L. Hoffman, I. S. Fletcher, and R. A. Duce, Further consideration of alkali and alkaline earth geochemistry of marine aerosols: results of a study of marine aerosols collected on Bermuda, Atmos. Environ., 11, 373-377, 1977.

Hogan, A. W., Continuing survey of maritime aerosols, Final Report, State University of New York at Albany, available from NTIS, Report No. PB-257,985, 1975.

Huebert, B. J. and A. L. Lazrus, Global tropospheric measurements of nitric acid vapor and particulate nitrate, Geophys. Res. Letters, 5, 577-580, 1978.

Huebert, B. J., A. L. Lazrus, A. C. Delany, An integrated system for aircraft sampling of remote-tropospheric aerosols and acidic gases, Paper presented at the 70th Annual Meeting, Air Pollution Control Association, Tornoto, Ontario, June 20-24, 1977.

Johansson, T. B., R. E. Van Grieken, J. W. Nelson, and J. W. Winchester, Elemental trace analysis of small samples by proton-induced X-ray emission, Anal. Chem., 47, 855-860, 1975.

Junge, C. E., The chemical composition of atmospheric aerosols: I measurements at Round Hill field station, June-July 1953, J. Meteorol., 11, 323-333, 1954.

Junge, C. E., Air Chemistry and Radioactivity, Academic Press, New York, 1963.

Lawson, D. R., Chemistry of the natural aerosol: A case study in South America, Ph.D. Thesis, Department of Oceanography, The Florida State University, 1978.

Liu, B. Y. H. and K. W. Lee, Efficiency of membrane and nuclepore filters for submicron aerosols, Environ. Sci. Tech., 10, 345-350, 1976.

Maenhaut, W., W. H. Zoller, R. A. Duce, and G. C. Hoffman, Concentration and size distribution of particle trace elements in the south polar atmosphere, J. Geophys. Res., 84, 2421-2431, 1979.

Mason, B. J., Principles of Geochemistry, 3rd edition, Wiley and Sons, New York, 1966.

Martens, C. S., Halogen chemistry of Puerto Rican and San Francisco Bay marine aerosols, J. Rech. Atmos., 8, 989-991, 1974.

Meinert, D. L. and J. W. Winchester, Chemical relationships in the North Atlantic marine aerosol, J. Geophys. Res., 82, 1778-1782, 1977.

Meszaros, A. and K. Vissy, Concentration, size distribution, and chemical nature of atmospheric aerosol particles in remote oceanic areas, Aerosol Sci., 5, 101-109, 1974.

Mitchell, R. I. and J. M. Pilcher, An improved cascade impactor for measuring aerosol particle sizes, Ind. and Eng. Chem., 51, 1039-1042, 1959.

Moore, D. J., Measurements of condensation nuclei over the North Atlantic, Quart. J. Roy. Meteorol. Soc., 78, 596-602, 1952.

Patterson, E. M., D. A. Gillette, and G. W. Grams, The relation between the visibility and the size-number distribution of airborne soil particles, J. Appl. Meteorol., 15, 470-478, 1976.

Patterson, E. M. and D. A. Gillette, Commonalities in measured size distributions for aerosol having a soil-derived component, J. Geophys. Res., 82, 2074-2082, 1977a.

Patterson, E. M. and D. A. Gillette, Measurements of visibility vs mass-concentration for airborne soil particles, Atmos. Environ., 11, 193-196, 1977b.

Pilat, M. J. and D. S. Ensor, Plume opacity and particulate mass concentration, Atmos. Environ., 4, 163-173, 1970.

Pilat, M. J. and D. S. Ensor, Comparison between the light extinction aerosol mass concentration relationships of atmosphere and air pollutant emission aerosols, Atmos. Environ., 5, 204-215, 1971.

Pinnick, R. G. and H. J. Auvermann, Response characteristics of Knollenberg light-scattering aerosol counters, J. Aerosol Sci., 10, 55-74, 1979.

Prospero, J. M., Mineral and sea salt aerosol concentrations in various ocean regions, J. Geophys. Res., 84, 725-731, 1979.

Rahn, K. A., Silicon and aluminum in atmospheric aerosols: Crust-air fractionation, Atm. Environ., 10, 597-601, 1976.

Rahn, K. A., G. E. Shaw, L. Schutz, and R. Jaenicke, Long-range impact of desert aerosol on atmospheric chemistry: Two examples, Paper presented at the Workshop on Saharan Dust Transport, Gothenberg, Sweden, 25-28 April 1977.

Spurney, K. R., J. P. Lodge, E. R. Frank, and D. C. Sheesley, Aerosol filtration by means of nuclepore filters-structural and filtration properties, Environ. Sci. Tech., 3, 453-464, 1969.

Sverdrup, G. M., K. T. Whitby, and W. E. Clark, Characterization of California aerosols, 2, Aerosol size distribution in the Mojave Desert, Atmos. Environ., 9, 483-494, 1975.

Vinogradov, A. P., The Geochemistry of Rare and Dispersed Chemical Elements in Soils, Translated from the Russian Consultants Bureau, New York, 1959.

Whitby, K. T., R. B. Husar, and B. Y. H. Liu, The aerosol size distribution of Los Angeles smog, in Aerosols and Atmospheric Chemistry, edited by G. M. Hidy, pp. 237-264, Academic Press, New York, 1972.

Wiellike, K., K. T. Whitby, W. E. Clark, and V. A. Marple, Size distribution of Denver aerosols - A comparison of two sites, Atmos. Environ., 8, 609-633, 1974.

Winchester, J. W. and R. A. Duce, Particulate matter exchange across the air-water interface, Proceedings of the Symposium on Fates of Pollutants in the Air and Water Environments, 169th National Meeting, American Chemical Society, Philadelphia, PA, 6-11 April 1975.

Winkler, P., The growth of atmospheric aerosol particles as a function of the relative humidity: II. An improved concept of mixed nucleii, Aerosol Sci., 4, 373-387, 1973.

Winkler, P., On production rates in marine aerosols in Proceedings of the Symposium on Radiation in the Atmosphere, H. J. Bolle, editor, Science Press, Princeton, 1977.

Winkler, P. and C. Junge, The growth of atmospheric aerosol particles as a function of the relative humidity: I Method and measurements at different locations, J. Rech. Atmos., 6, 617-638, 1972.

Woodcock, A. H., Salt nucleii in marine air as a function of altitude and wind force, J. Meteorol., 10, 362-371, 1953.

Woodcock, A. H., Smaller salt particles in oceanic air and bubble behavior in the sea, J. Geophys. Res., 77, 5316-5321, 1972.

Table 1. Enrichment Factors for the Large Particle Mode of the Continental Aerosol.

Location	Al	Si	Ca	Ti	K	Fe
Boundary Layer, Southwestern U.S.	1.1	0.7	1.6	1.1	1.3	1.0
Free Troposphere, Southwestern U.S.	1.6	0.8	1.9	1.0	1.5	1.0
Free Troposphere, Western U.S.	1.5	0.7	2.4	-	1.2	1.0
Free Troposphere, Pacific Ocean West of U.S.	1.0	0.9	3.3	1.1	1.3	1.0

Calculated using crustal abundance data of Mason, 1966, relative to Fe.

FIGURE CAPTIONS

1. Flight tracks for Electra aircraft during the 1977 (solid line) and 1978 (dashed line) flight patterns.

2. Two typical size-number distributions measured over the southwestern continental United States. The solid line represents a size distribution measured within the boundary layer, and the dashed line represents a free-tropospheric size distribution. The curves in each case are fits to log-normal distributions.

3. A representative temperature-dew point-aerosol sounding from the southwestern continental United States. Aerosol number concentrations are presented as relative number concentration for large ($r > 0.5$ μm) and for small ($r < 0.5$ μm) particles. The boundary layer at the time of this sounding was estimated to extend up to approximately 2.7 km, although there is evidence of significant mixing from the surface up to approximately 5 km.

4. Typical time sequence plots for continental aerosol properties for the 22 August 1977 flight from Denver to San Francisco. Panel (a) gives the aircraft altitude in kilometers above sea level; panel (b), the particle number as measured with the PMS optical probes. The small-particle number is the total particle number for $0.15 < r < 0.5$ μm; the large particle number is that for $r > 0.5$ μm. Panel (c) shows the calculated extinction for the two size ranges using the indicated optical properties and the PMS distribution; panel (d) gives the calculated mass for each range assuming a specific gravity of 2. The time period from 20:50 to 22:00 represents boundary layer data; the rest is free-tropospheric data. Data is omitted with the aircraft penetrated clouds.

5. Two typical marine size distributions expressed as a number distribution (a) and a volume distribution (b). The figures show the very large increase in particle number and volume upon entering the marine boundary layer.

6. A representative temperature-dew point-aerosol sounding from the marine measurements over the Pacific. The sounding shows the rapid decrease in both large and small particle counts on going from the marine boundary layer to the marine free-troposphere at $\sim$2 km.

7. Three measured GAMETAG marine boundary layer size distributions for the indicated Beaufort wind forces are shown by the solid lines in the figure; the data of Woodcock (1953) are shown by the dashed line. The Woodcock data are for a wind of Beaufort force 5.

8. A comparison of the sea salt concentrations inferred from the PMS optical particle counter data and the chemical measurements. The dashed line represents the line of equal concentrations by each method. See text for details of the comparison.

9. Calculated total dry sea salt concentration plotted against wind force for the 1977 (x) data and the 1978 (+) data. Also shown on the figure adapted from Junge (1963) are the lines forming an envelope for Woodcock's data as well as data of Junge (·····) and Moore (⊕) for salt concentration as a function of wind force. See text for details of the dry salt determination from the optical data.

10. Small-particle volume plotted as a function of the large-particle volume as measured with the PMS optical particle counters. The dashed line represents a linear least-squares fit to the data.

11. Elemental Cl concentration determined from the measured Ca concentrations plotted against the directly measured elemental Cl concentrations for our Pacific MBL samples. The data are consistent with the loss of Cl in the aerosol sample.

12. Data of Huebert et al. (this issue) for sulfate vs chloride concentrations measured during the 1978 GAMETAG flight series over the Pacific Ocean. The circled data point shows a high concentration of sulfate relative to the chloride, which we have interpreted as being indicative of gas-to-particle conversion over the ocean.

13. A GAMETAG marine boundary layer size distribution for the circled data point of Fig. 15 inferred on the basis of the PMS data and the chemical data as described in the text. A major portion of the small-particle volume is associated with particles with $r < 0.1$ μm, which we attribute to locally produced secondary aerosols.

14. Two free-tropospheric size distributions showing the variability (by approximately an order of magnitude) in the number of small particles measured in two samples separated by approximately 100 km.

15. Same as Fig. 8, except for marine aerosols.

16. Total aerosol volume plotted against latitude along the aircraft flight track for the marine boundary layer data for the 1977 (x) and 1978 (+) flights.

17. Small particle mass (a) and total particle mass (b) for the MFT measurements plotted against latitude along the aircraft flight track for the 1977 (x) and 1978(+) data.

18. Measured Fe concentration plotted against latitude along the aircraft flight track for the 1978 GAMETAG flights. The horizontal line is drawn to cover the latitude range of the sample; the vertical lines for each sample represent the error bounds associated with each measured concentration.

19. Calculated optical extinction for the 1977 (x) and 1978 (+) MFT data plotted as a function of latitude. See text for details.

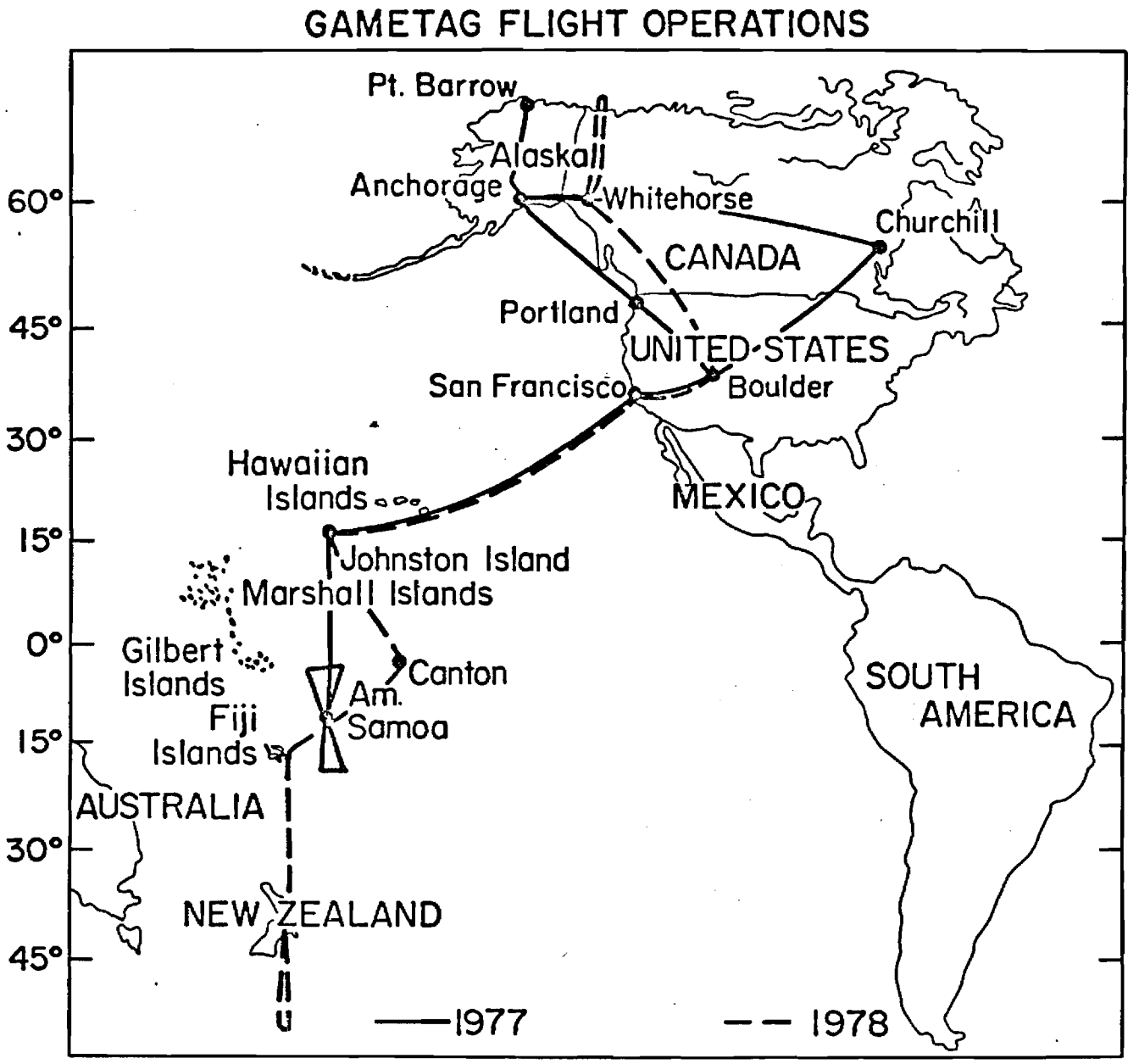
GAMETAG FLIGHT OPERATIONS
Pt. Barrow
Alaska
Anchorage
Whitehorse
Churchill
CANADA
Portland
UNITED STATES
San Francisco
Boulder
Hawaiian Islands
MEXICO
Johnston Island
Marshall Islands
Gilbert Islands
Canton
Am. Samoa
Fiji Islands
SOUTH AMERICA
AUSTRALIA
NEW ZEALAND
60°
45°
30°
15°
0°
15°
30°
45°
1977
1978

Fig. 1

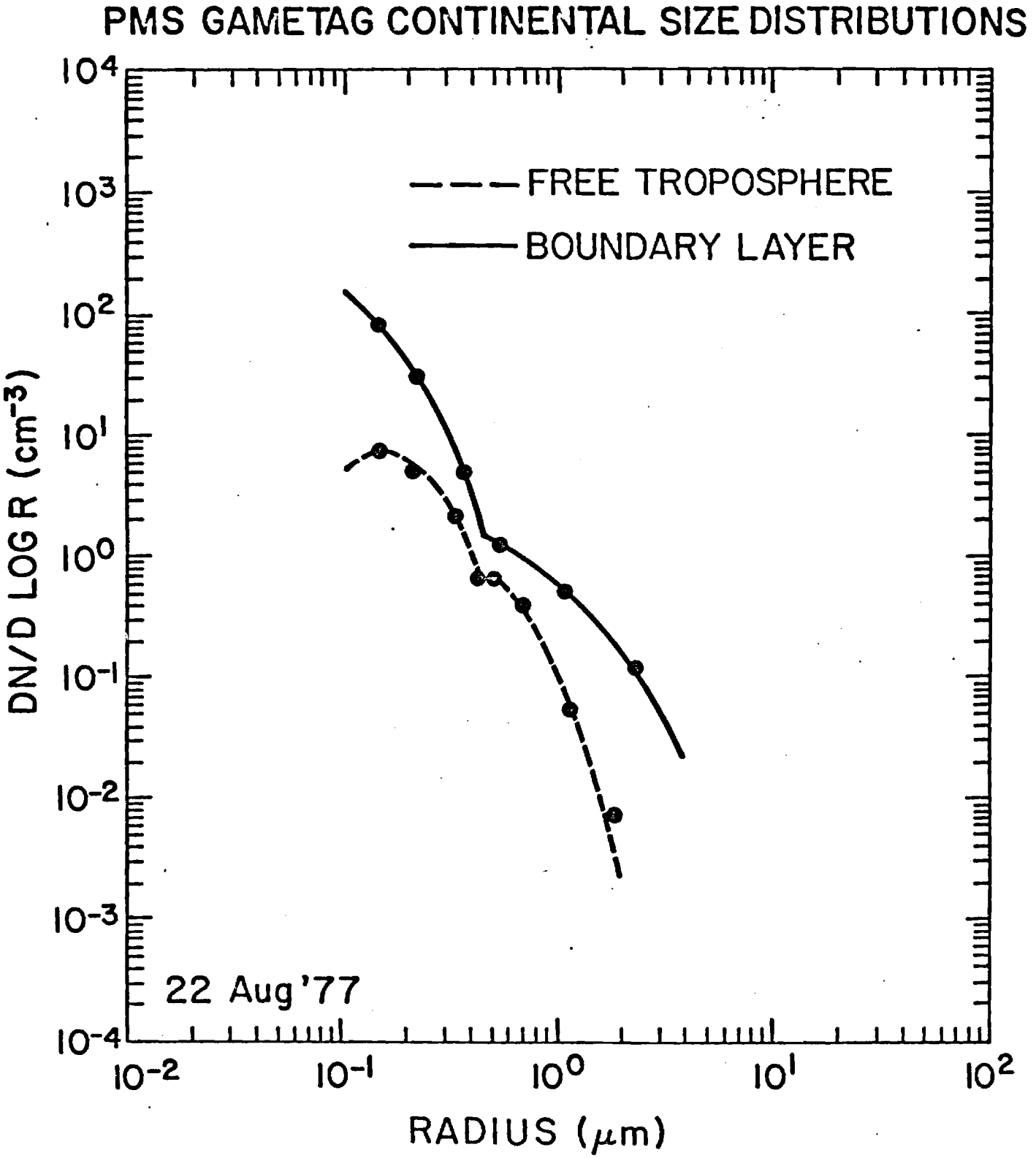
PMS GAMETAG CONTINENTAL SIZE DISTRIBUTIONS
FREE TROPOSPHERE
BOUNDARY LAYER
22 Aug '77
DN/D LOG R (cm⁻³)
RADIUS (μm)
10⁴
10³
10²
10¹
10⁰
10⁻¹
10⁻²
10⁻³
10⁻⁴
10⁻²
10⁻¹
10⁰
10¹
10²

Fig. 2

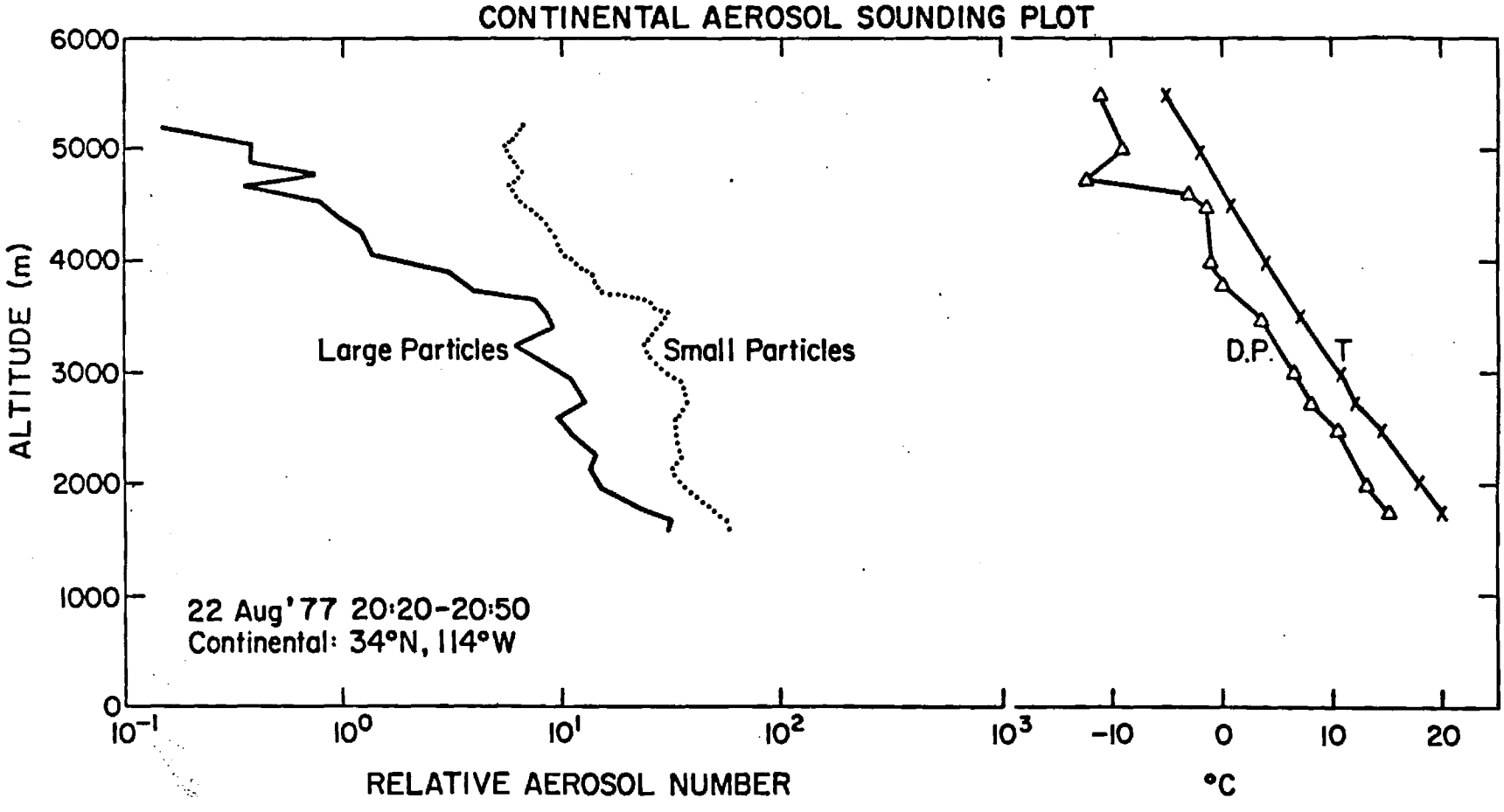
CONTINENTAL AEROSOL SOUNDING PLOT
ALTITUDE (m)
6000
5000
4000
3000
2000
1000
0
Large Particles
Small Particles
D.P.
T
22 Aug'77 20:20-20:50
Continental: 34°N, 114°W
10^{-1}
10^{0}
10^{1}
10^{2}
10^{3}
RELATIVE AEROSOL NUMBER
-10
0
10
20
°C

Fig. 3

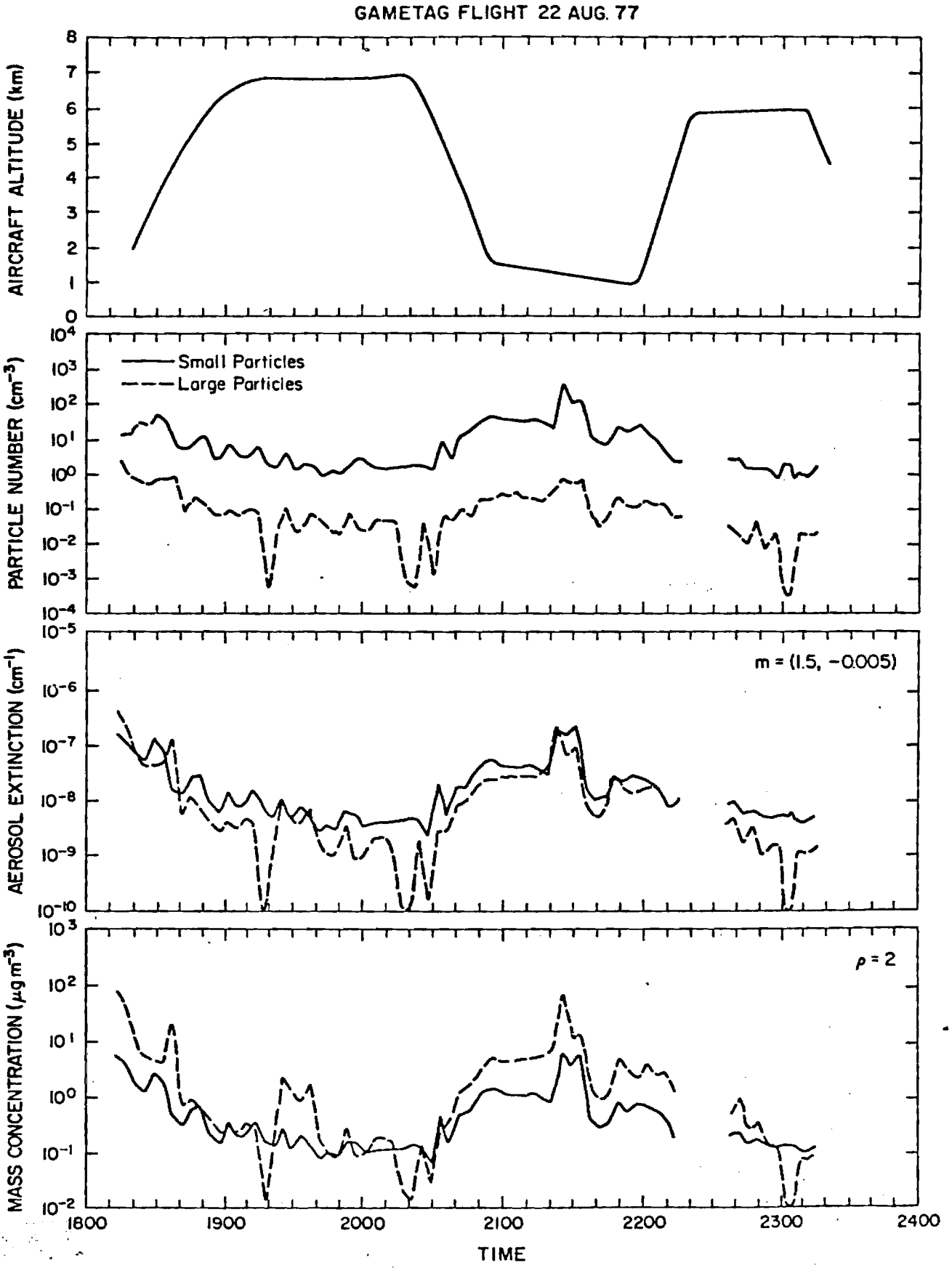
GAMETAG FLIGHT 22 AUG. 77
AIRCRAFT ALTITUDE (km)
PARTICLE NUMBER (cm⁻³)
Small Particles
Large Particles
AEROSOL EXTINCTION (cm⁻¹)
m = (1.5, −0.005)
MASS CONCENTRATION (μg m⁻³)
ρ = 2
TIME

Fig. 4

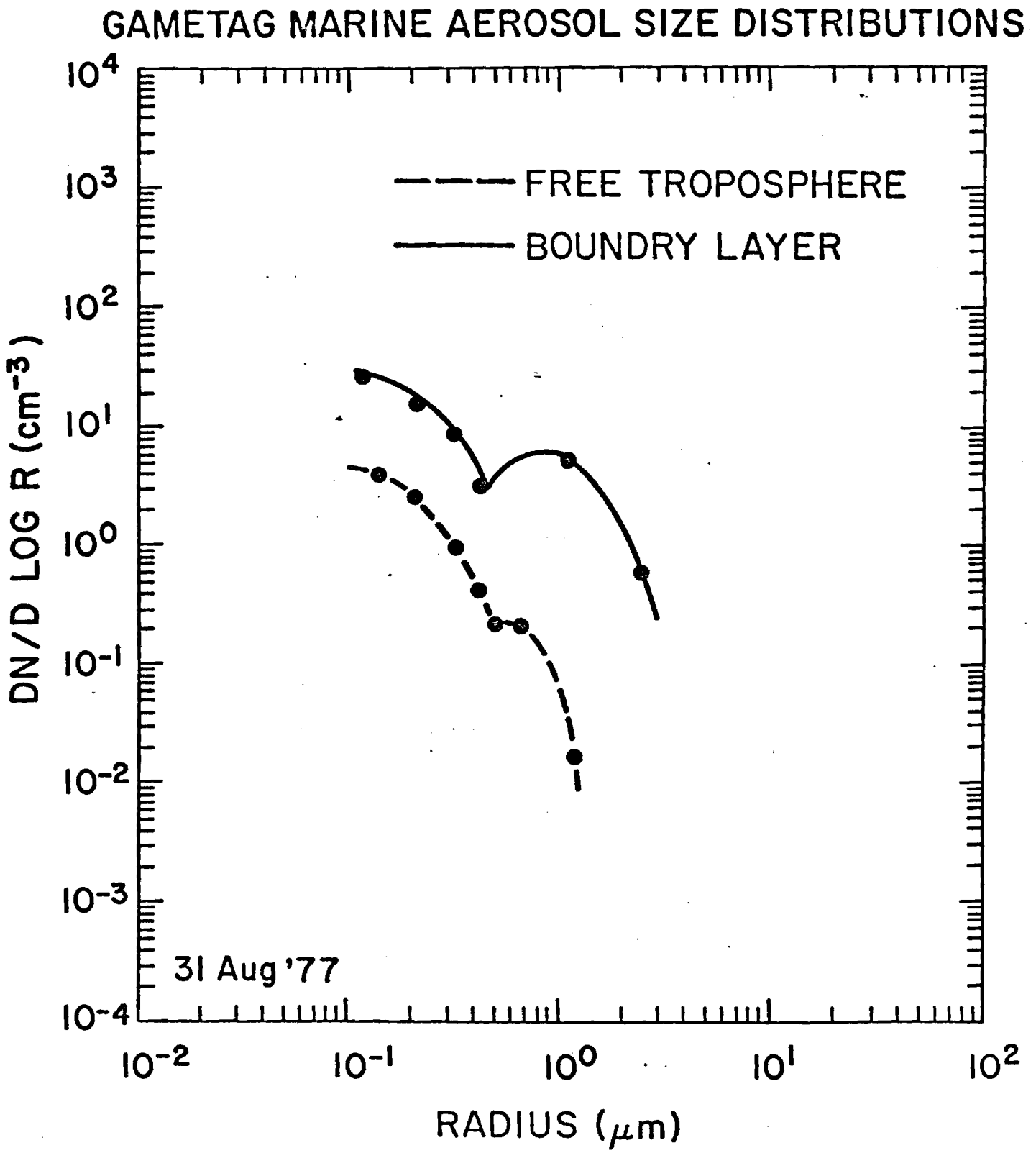
GAMETAG MARINE AEROSOL SIZE DISTRIBUTIONS
FREE TROPOSPHERE
BOUNDRY LAYER
31 Aug '77
DN/D LOG R (cm⁻³)
RADIUS (μm)
10⁴
10³
10²
10¹
10⁰
10⁻¹
10⁻²
10⁻³
10⁻⁴
10⁻²
10⁻¹
10⁰
10¹
10²

Fig. 5a

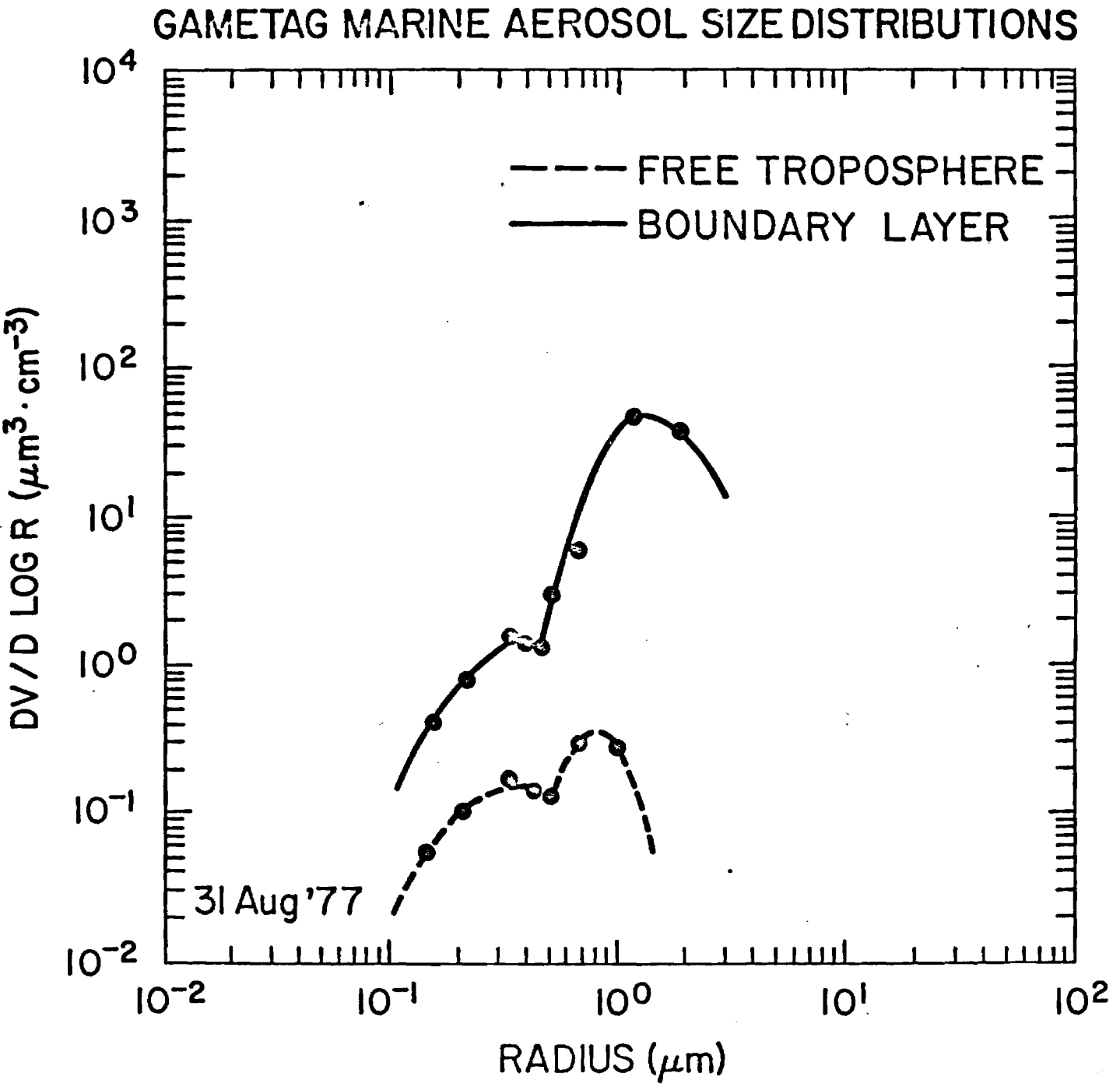
GAMETAG MARINE AEROSOL SIZE DISTRIBUTIONS
FREE TROPOSPHERE
BOUNDARY LAYER
31 Aug '77
DV/D LOG R (μm³·cm⁻³)
RADIUS (μm)
10⁴
10³
10²
10¹
10⁰
10⁻¹
10⁻²
10⁻²
10⁻¹
10⁰
10¹
10²

Fig. 5b

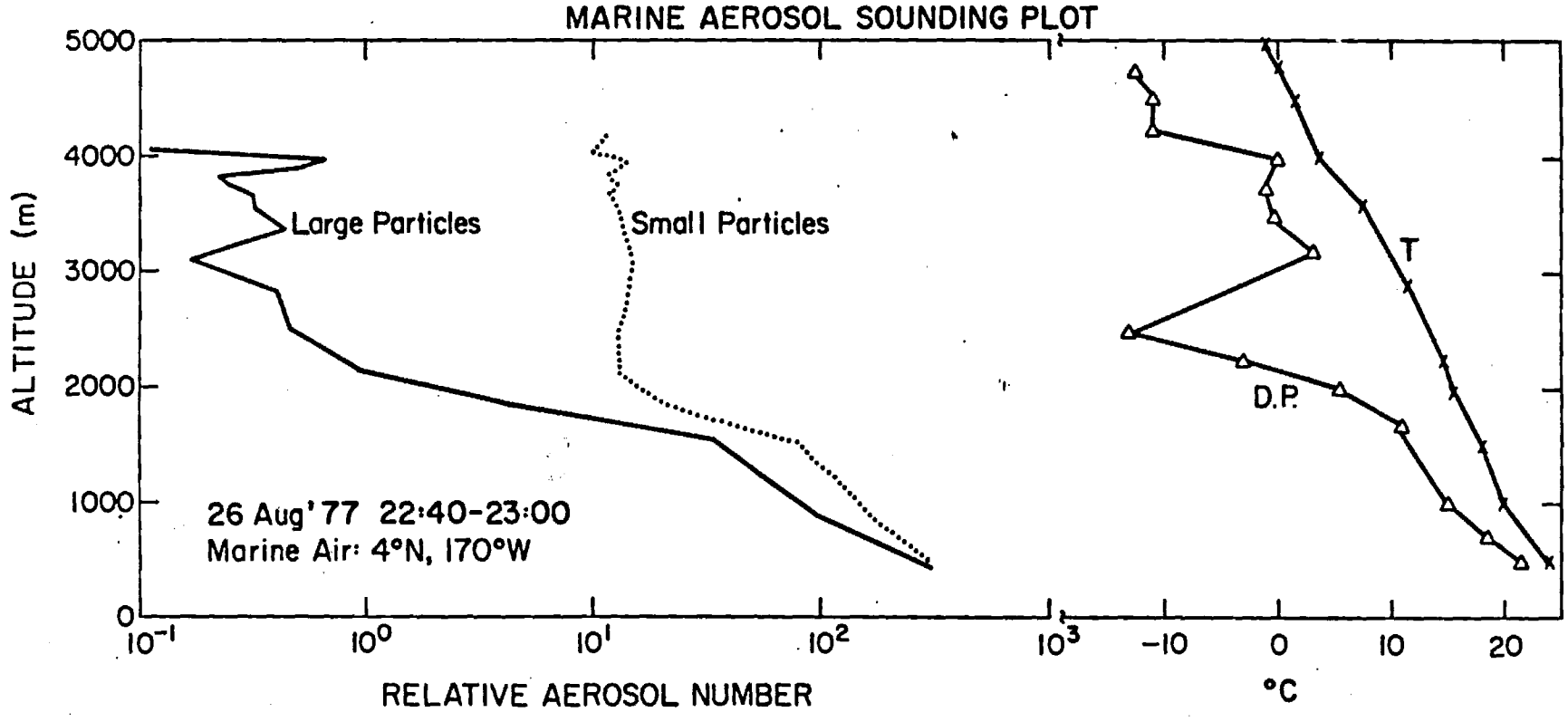
MARINE AEROSOL SOUNDING PLOT
ALTITUDE (m)
5000
4000
3000
2000
1000
0
Large Particles
Small Particles
T
D.P.
26 Aug'77 22:40-23:00
Marine Air: 4°N, 170°W
10^{-1}
10^{0}
10^{1}
10^{2}
10^{3}
RELATIVE AEROSOL NUMBER
−10
0
10
20
°C

Fig. 6

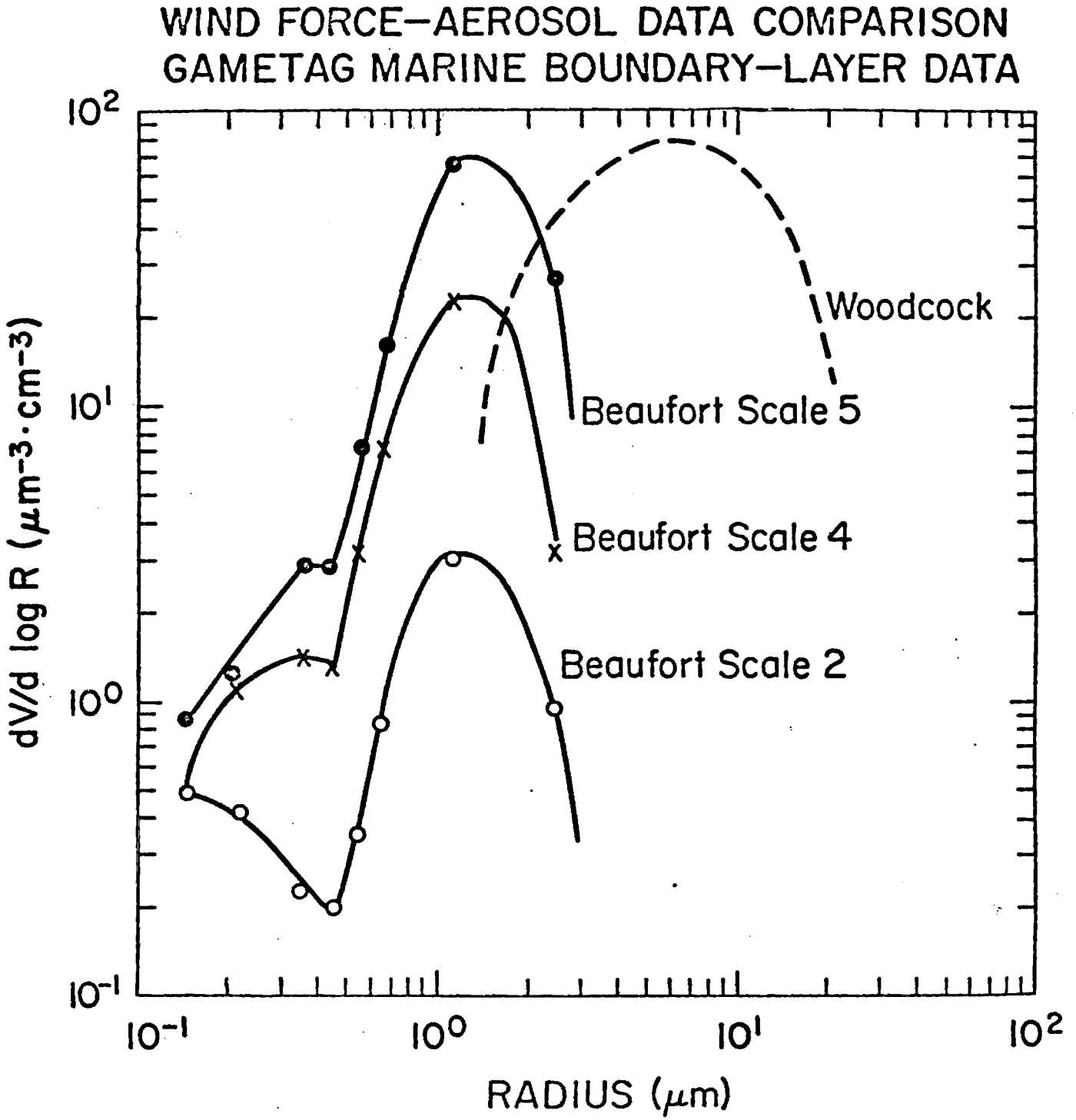
WIND FORCE–AEROSOL DATA COMPARISON
GAMETAG MARINE BOUNDARY–LAYER DATA
dV/d log R (μm⁻³·cm⁻³)
RADIUS (μm)
Woodcock
Beaufort Scale 5
Beaufort Scale 4
Beaufort Scale 2

Fig. 7

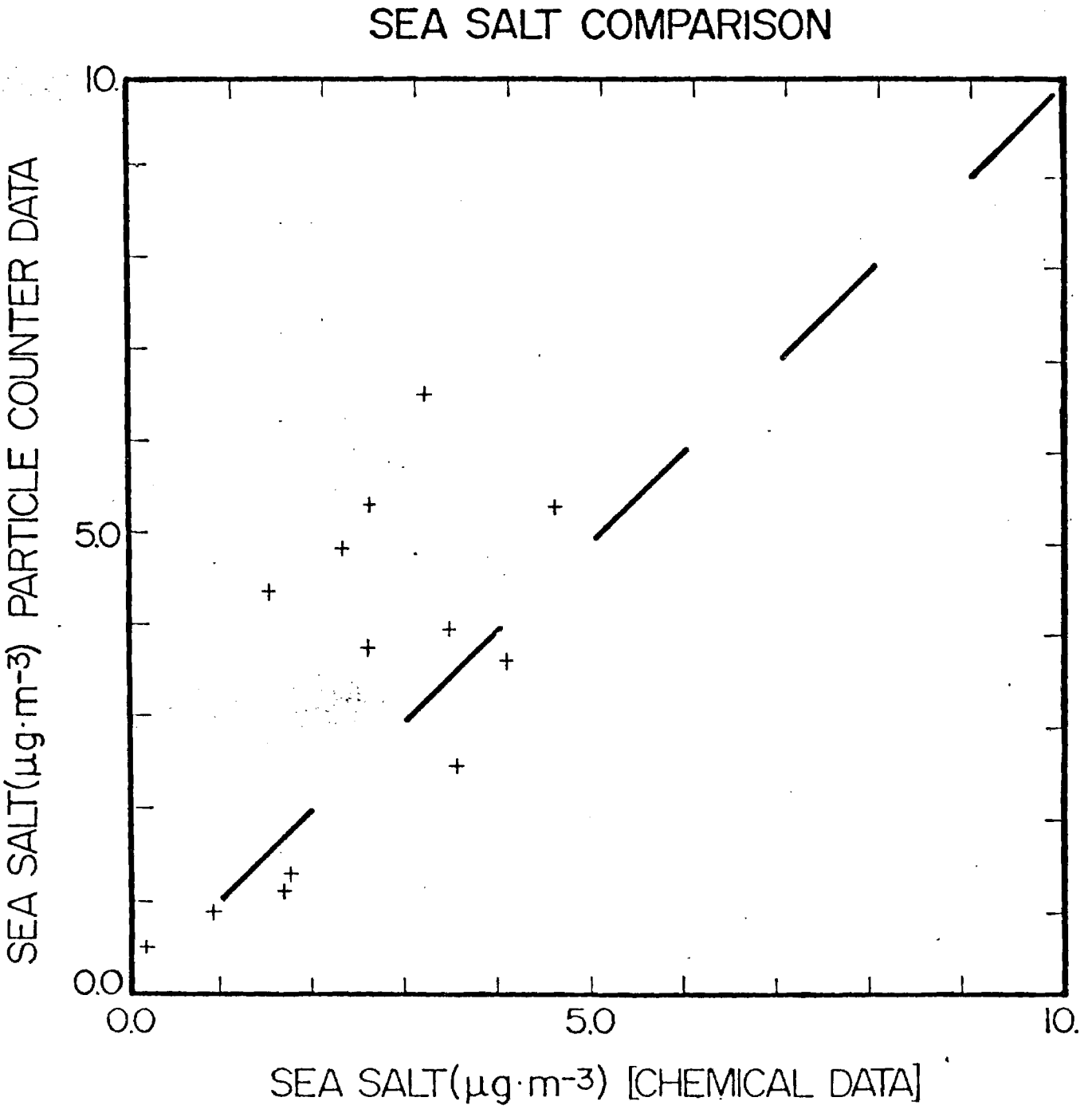
SEA SALT COMPARISON
10.
5.0
0.0
0.0
5.0
10.
SEA SALT(μg·m-3) PARTICLE COUNTER DATA
SEA SALT(μg·m-3) [CHEMICAL DATA]

Fig. 8

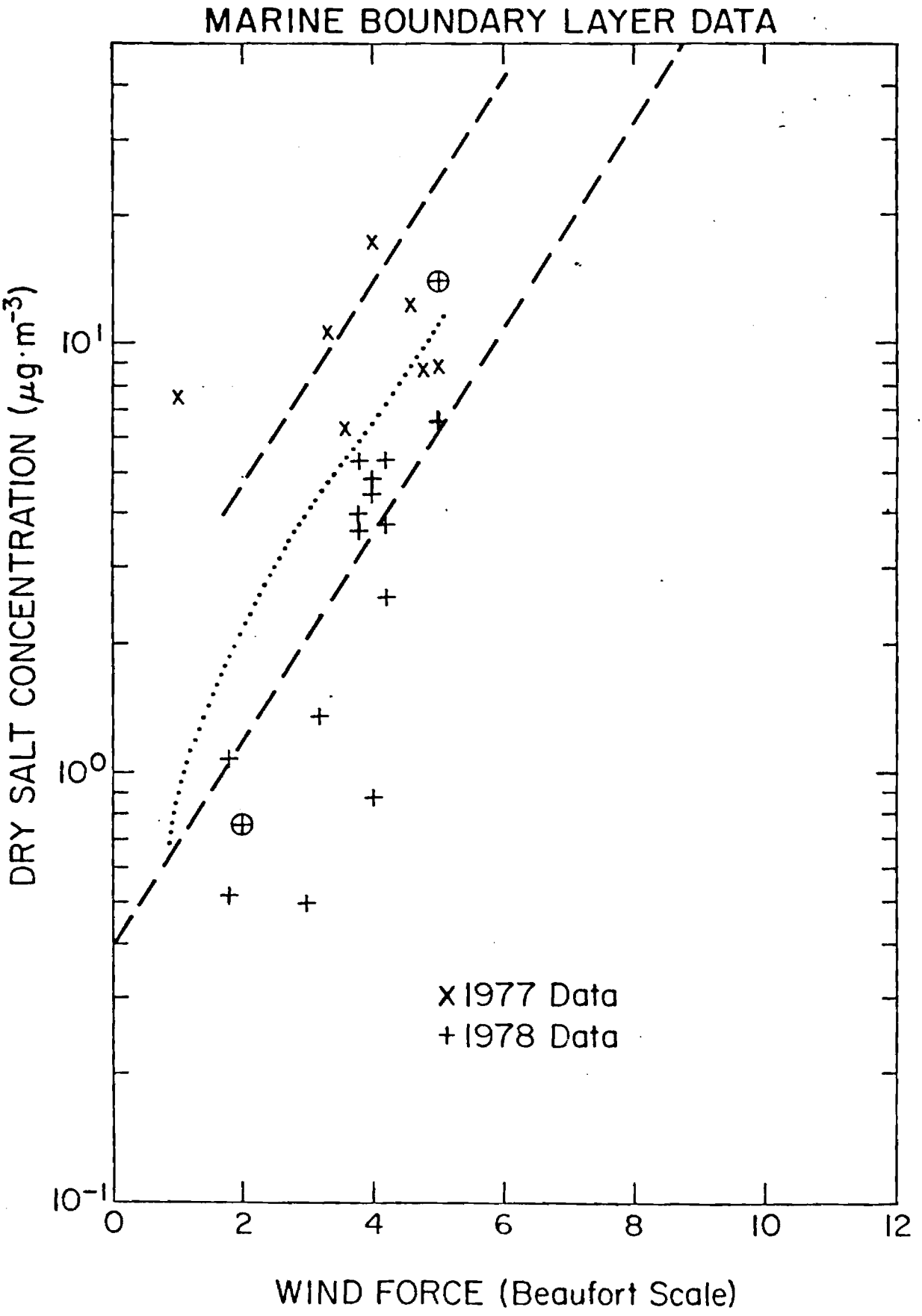
MARINE BOUNDARY LAYER DATA
DRY SALT CONCENTRATION ($\mu g \cdot m^{-3}$)
10^1
10^0
10^{-1}
0
2
4
6
8
10
12
WIND FORCE (Beaufort Scale)
x 1977 Data
+ 1978 Data

Fig. 9

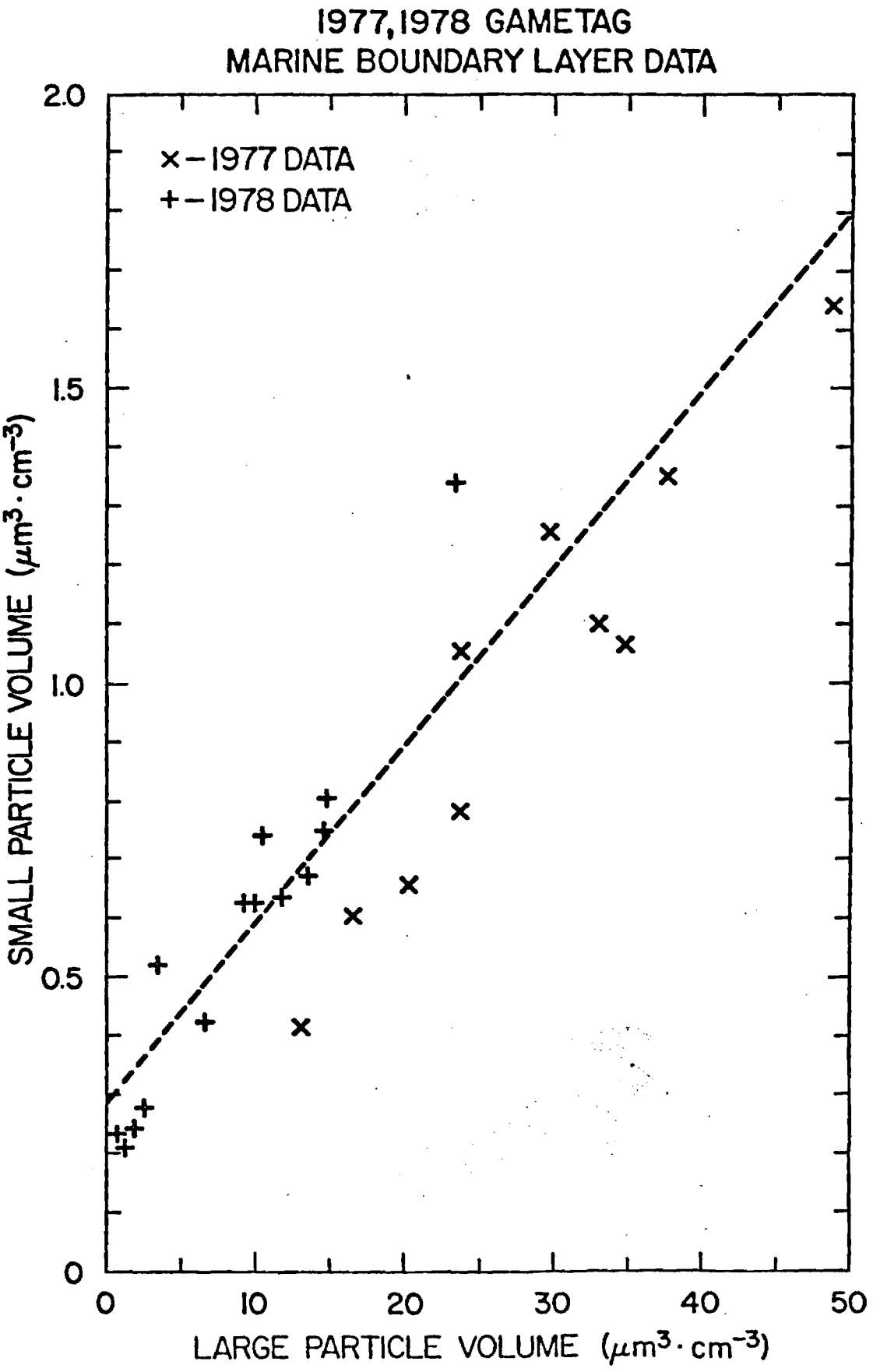
1977,1978 GAMETAG
MARINE BOUNDARY LAYER DATA
× – 1977 DATA
+ – 1978 DATA
SMALL PARTICLE VOLUME (μm³·cm⁻³)
LARGE PARTICLE VOLUME (μm³·cm⁻³)
0
0.5
1.0
1.5
2.0
0
10
20
30
40
50

Fig. 10

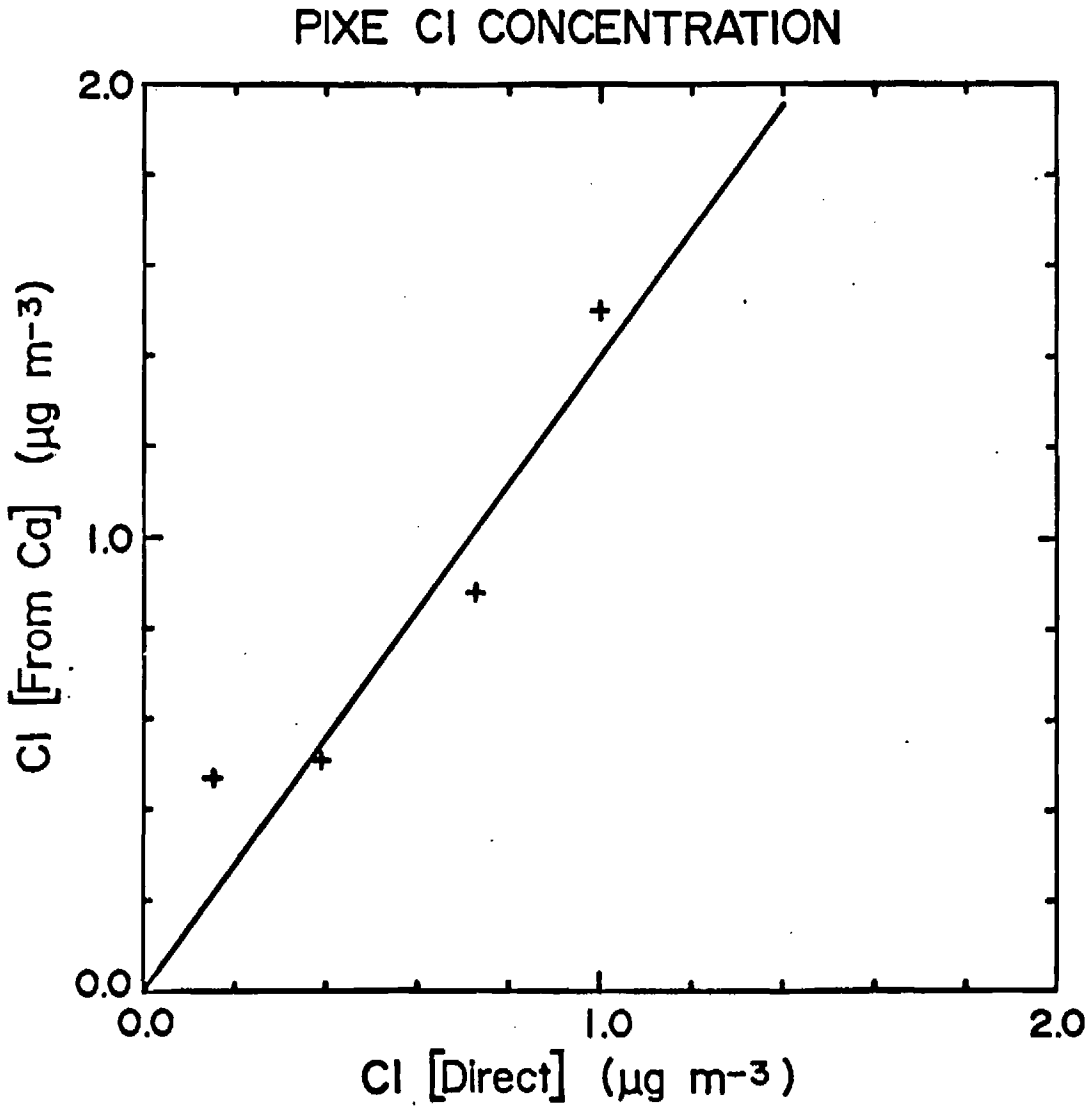
PIXE Cl CONCENTRATION
2.0
1.0
0.0
0.0
1.0
2.0
Cl [From Ca] (μg m-3)
Cl [Direct] (μg m-3)

Fig. 11

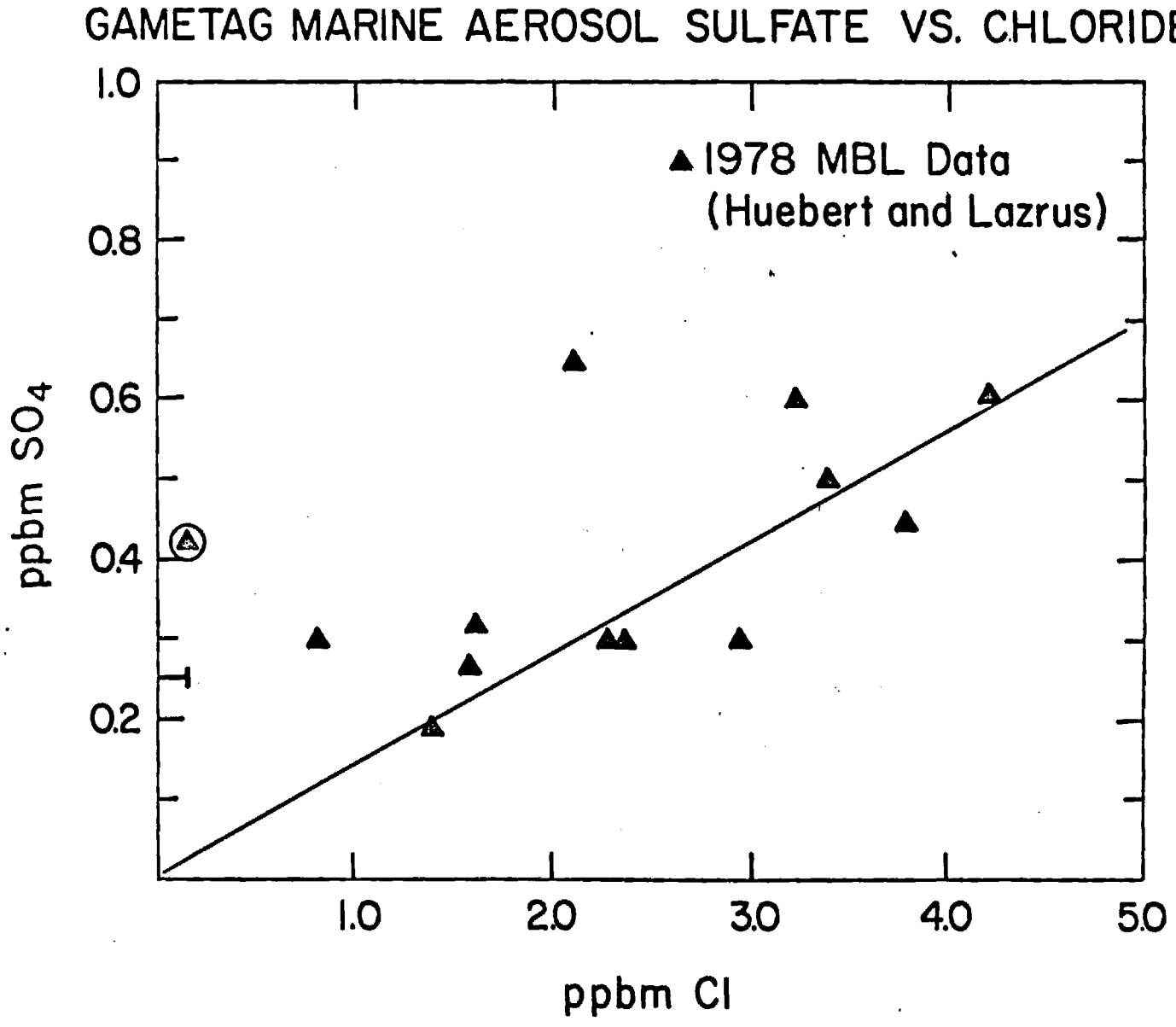
GAMETAG MARINE AEROSOL SULFATE VS. CHLORIDE
1978 MBL Data
(Huebert and Lazrus)
ppbm SO4
ppbm Cl
1.0
0.8
0.6
0.4
0.2
1.0
2.0
3.0
4.0
5.0

Fig. 12

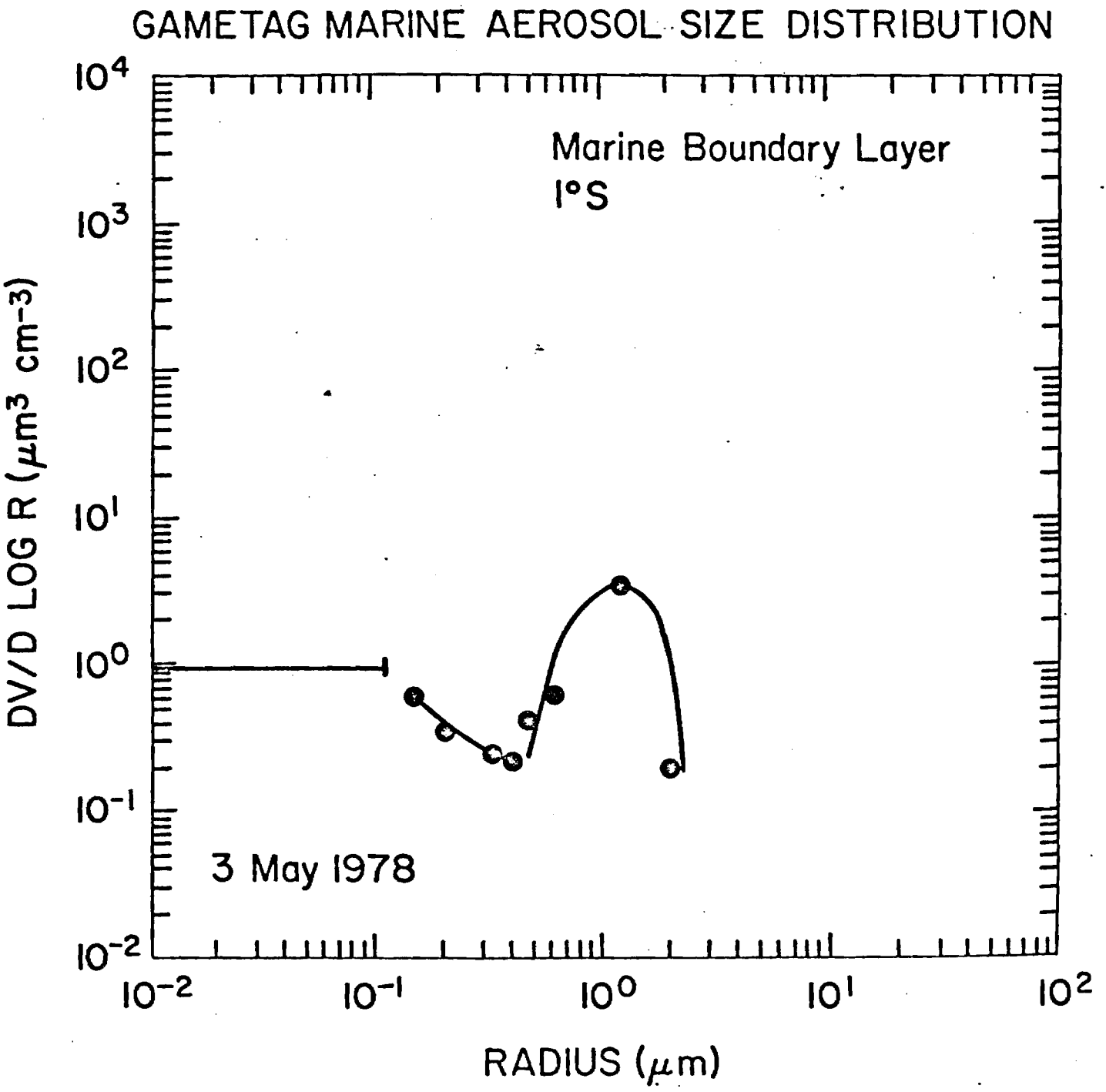
GAMETAG MARINE AEROSOL SIZE DISTRIBUTION
Marine Boundary Layer
1°S
3 May 1978
DV/D LOG R (μm³ cm⁻³)
RADIUS (μm)
10⁴
10³
10²
10¹
10⁰
10⁻¹
10⁻²
10⁻²
10⁻¹
10⁰
10¹
10²

Fig. 13

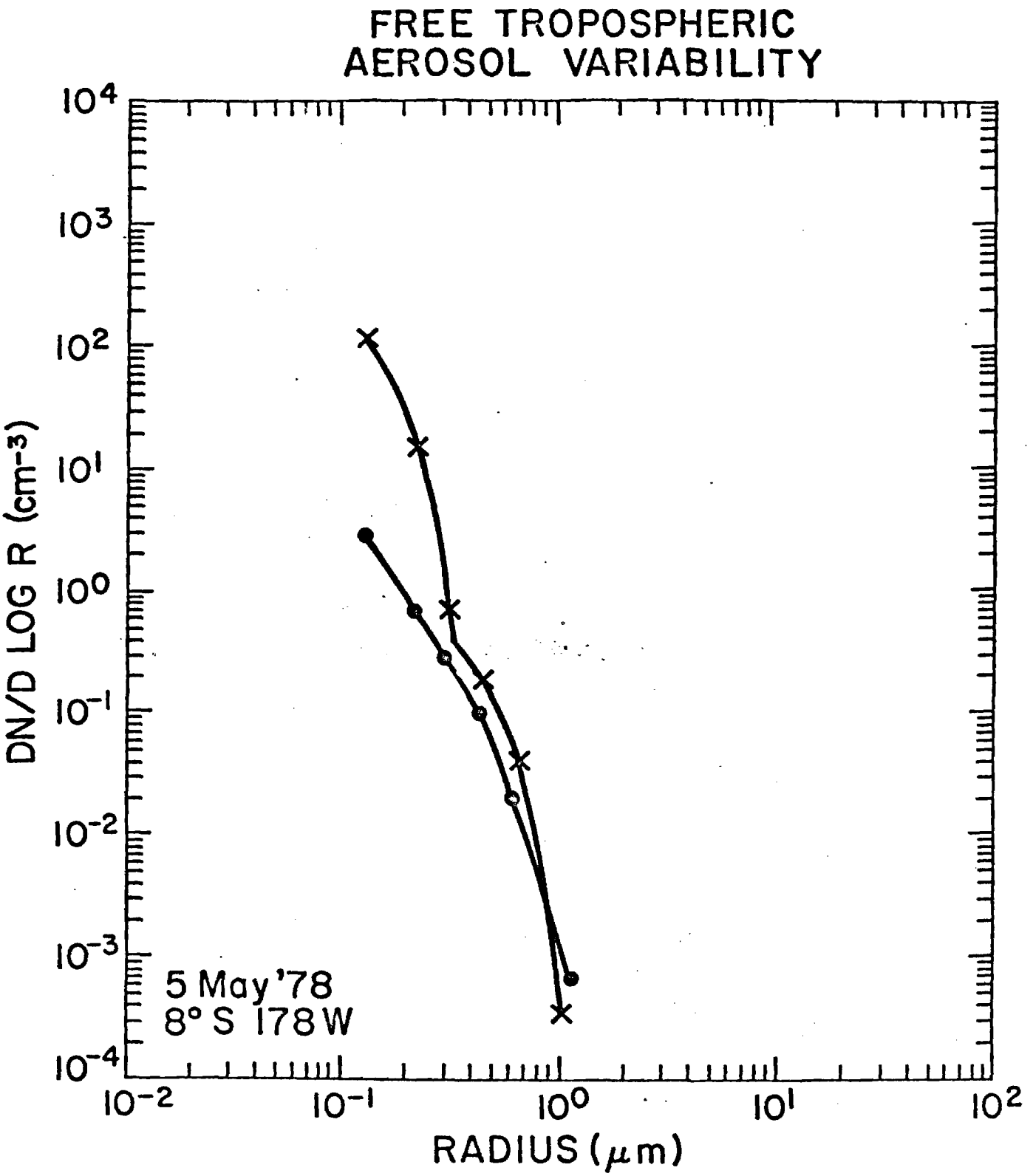
FREE TROPOSPHERIC
AEROSOL VARIABILITY
DN/D LOG R (cm-3)
RADIUS (μm)
5 May '78
8° S 178 W
10^4
10^3
10^2
10^1
10^0
10^-1
10^-2
10^-3
10^-4
10^-2
10^-1
10^0
10^1
10^2

Fig. 14

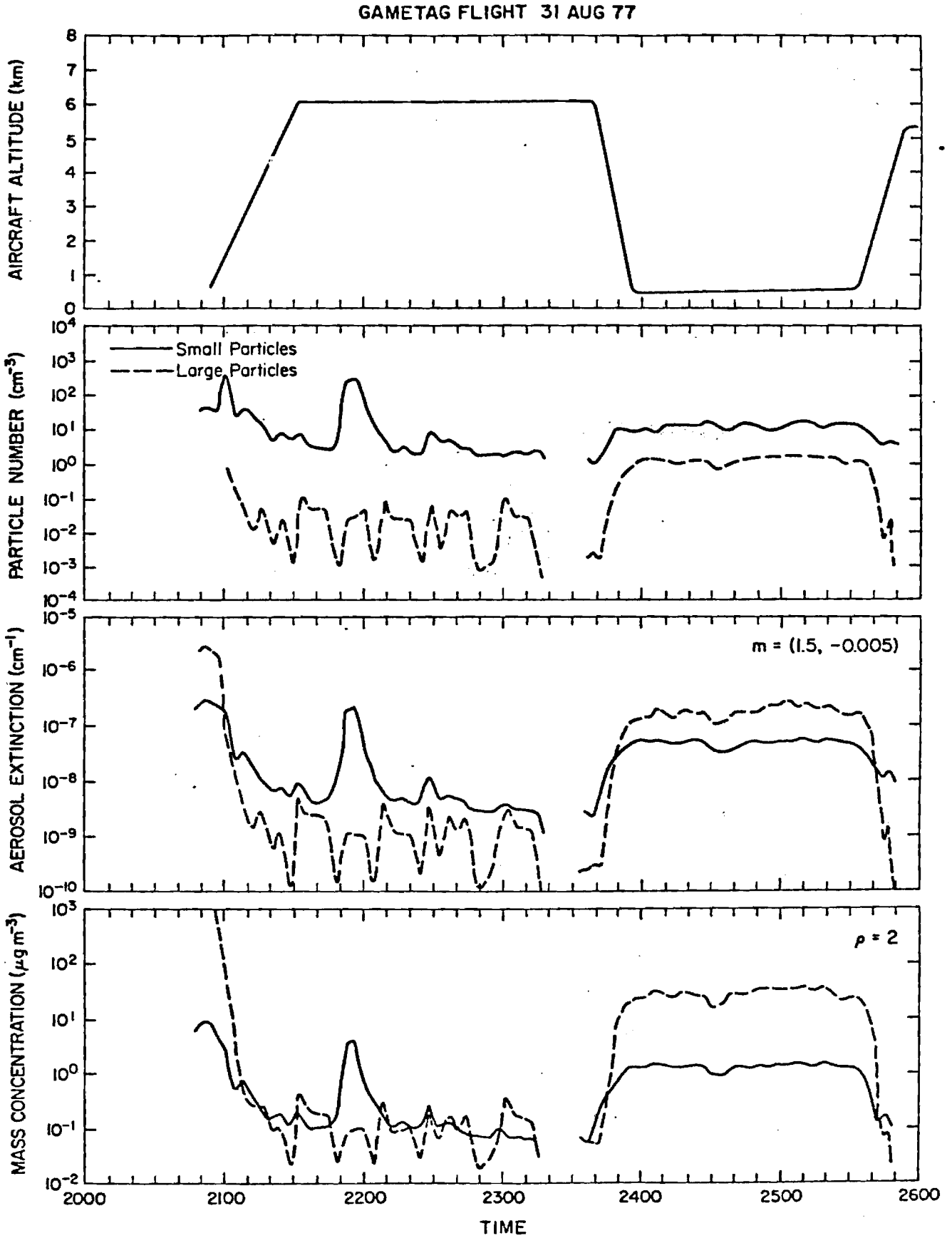
GAMETAG FLIGHT 31 AUG 77
AIRCRAFT ALTITUDE (km)
PARTICLE NUMBER (cm⁻³)
Small Particles
Large Particles
AEROSOL EXTINCTION (cm⁻¹)
m = (1.5, -0.005)
MASS CONCENTRATION (μg m⁻³)
ρ = 2
TIME

Fig. 15

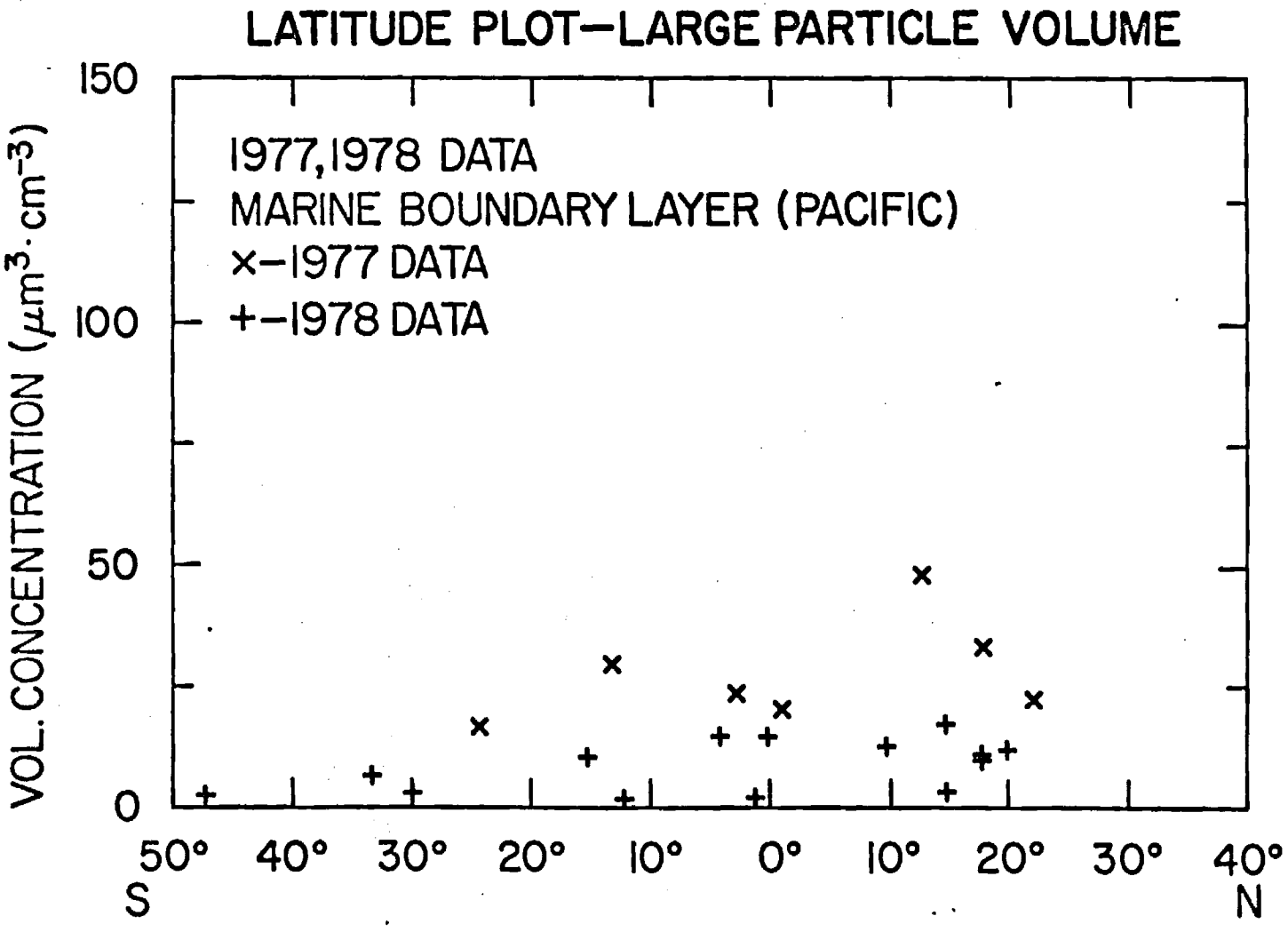
LATITUDE PLOT—LARGE PARTICLE VOLUME
1977,1978 DATA
MARINE BOUNDARY LAYER (PACIFIC)
×—1977 DATA
+—1978 DATA
VOL. CONCENTRATION (μm³·cm⁻³)
150
100
50
0
50°
40°
30°
20°
10°
0°
10°
20°
30°
40°
S
N

Fig. 16

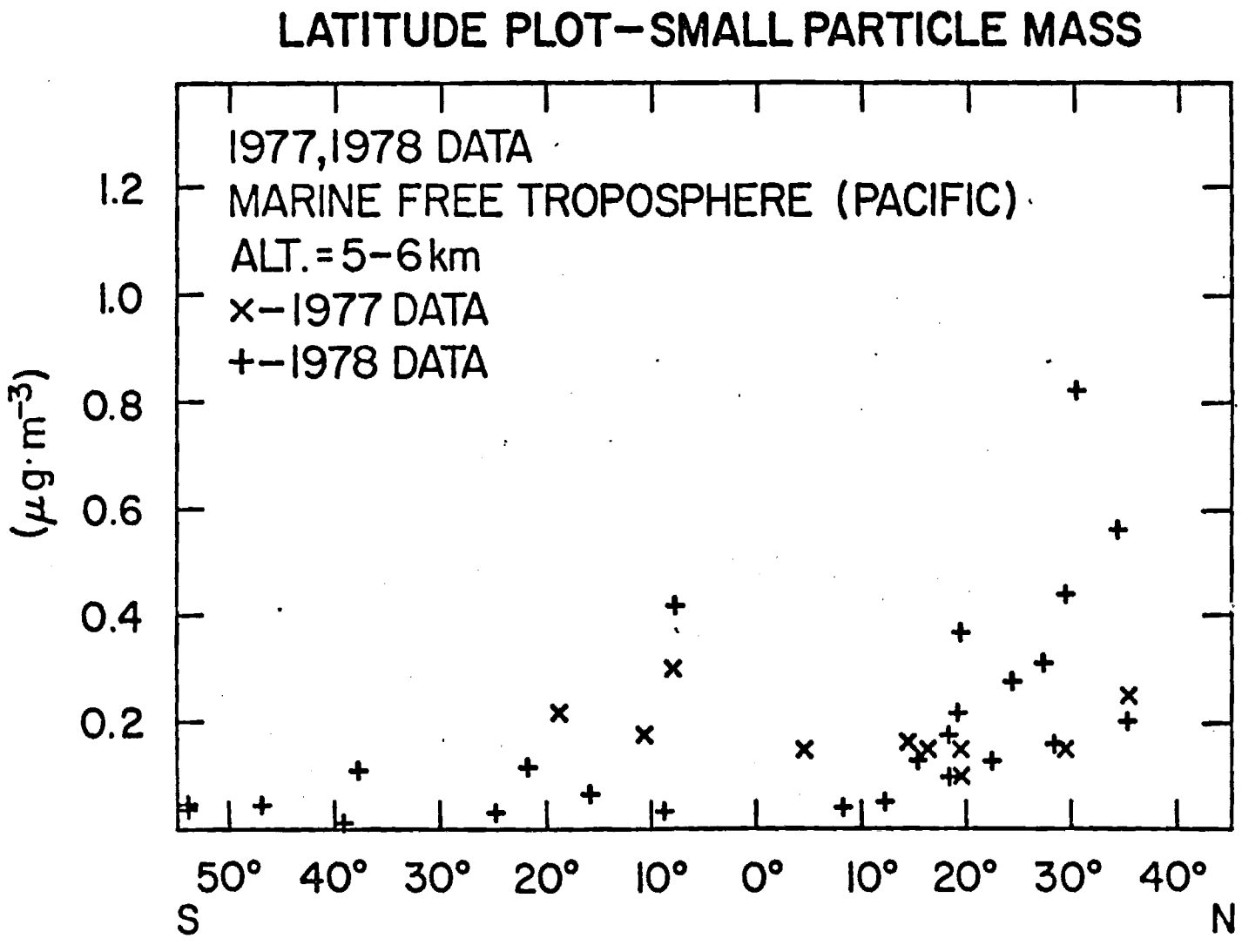
LATITUDE PLOT–SMALL PARTICLE MASS
1977,1978 DATA
MARINE FREE TROPOSPHERE (PACIFIC)
ALT.=5–6km
×–1977 DATA
+–1978 DATA
(μg·m⁻³)
1.2
1.0
0.8
0.6
0.4
0.2
50° 40° 30° 20° 10° 0° 10° 20° 30° 40°
S
N

Fig. 17a

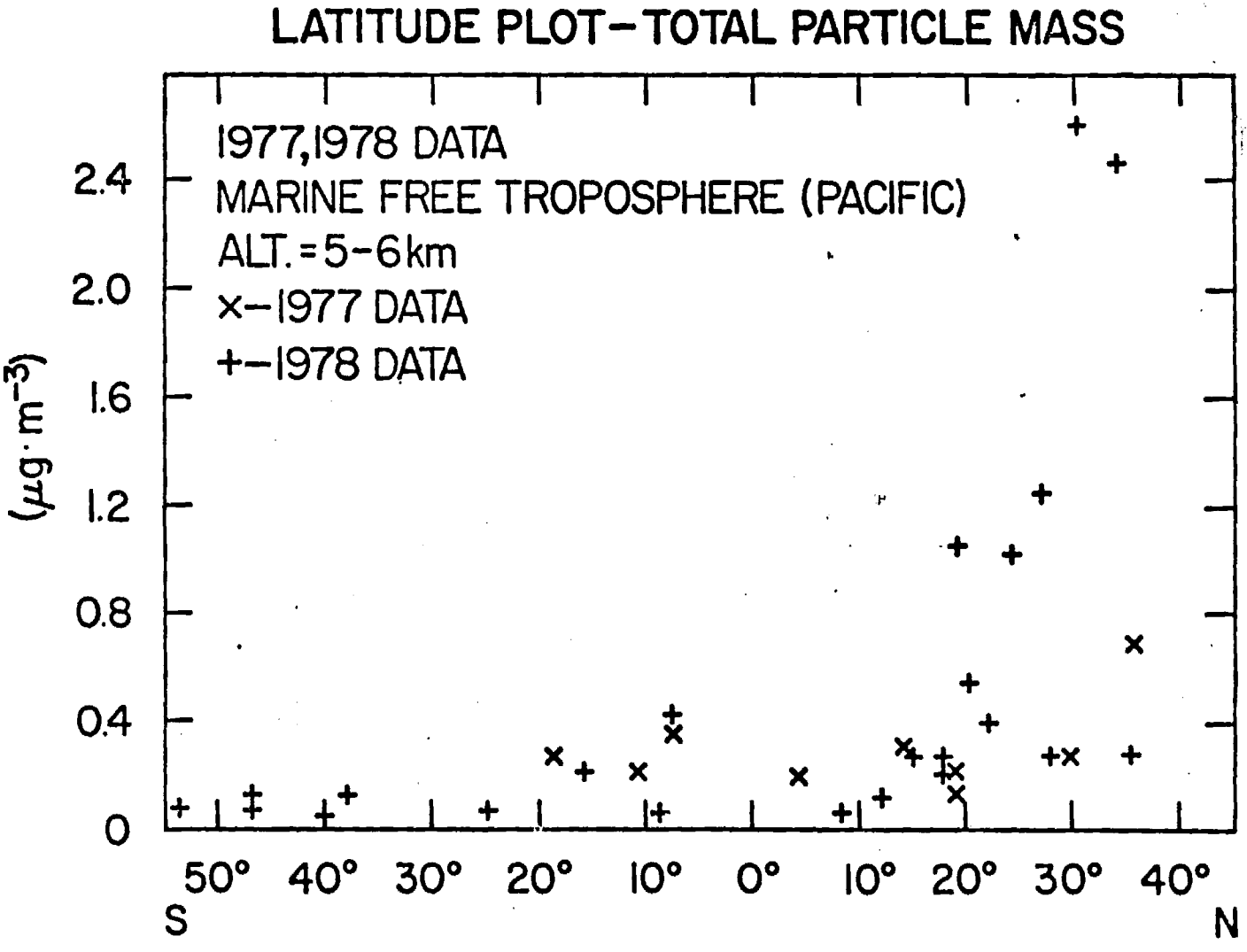
LATITUDE PLOT–TOTAL PARTICLE MASS
1977,1978 DATA
MARINE FREE TROPOSPHERE (PACIFIC)
ALT.=5–6km
×–1977 DATA
+–1978 DATA
(μg·m⁻³)
2.4
2.0
1.6
1.2
0.8
0.4
0
50° 40° 30° 20° 10° 0° 10° 20° 30° 40°
S
N

Fig. 17b

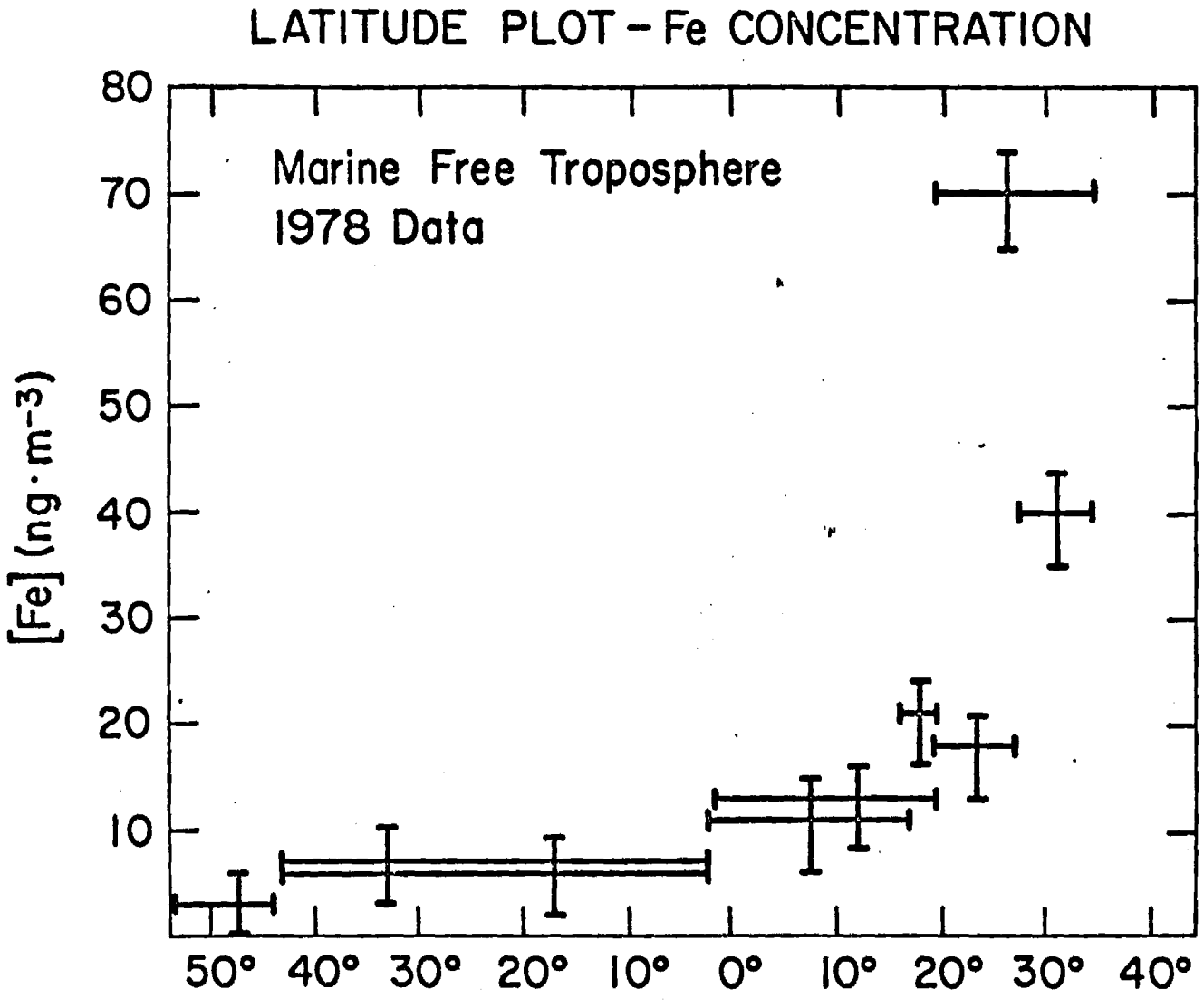
LATITUDE PLOT - Fe CONCENTRATION
Marine Free Troposphere
1978 Data
[Fe] (ng·m⁻³)
80
70
60
50
40
30
20
10
50° 40° 30° 20° 10° 0° 10° 20° 30° 40°

Fig. 18

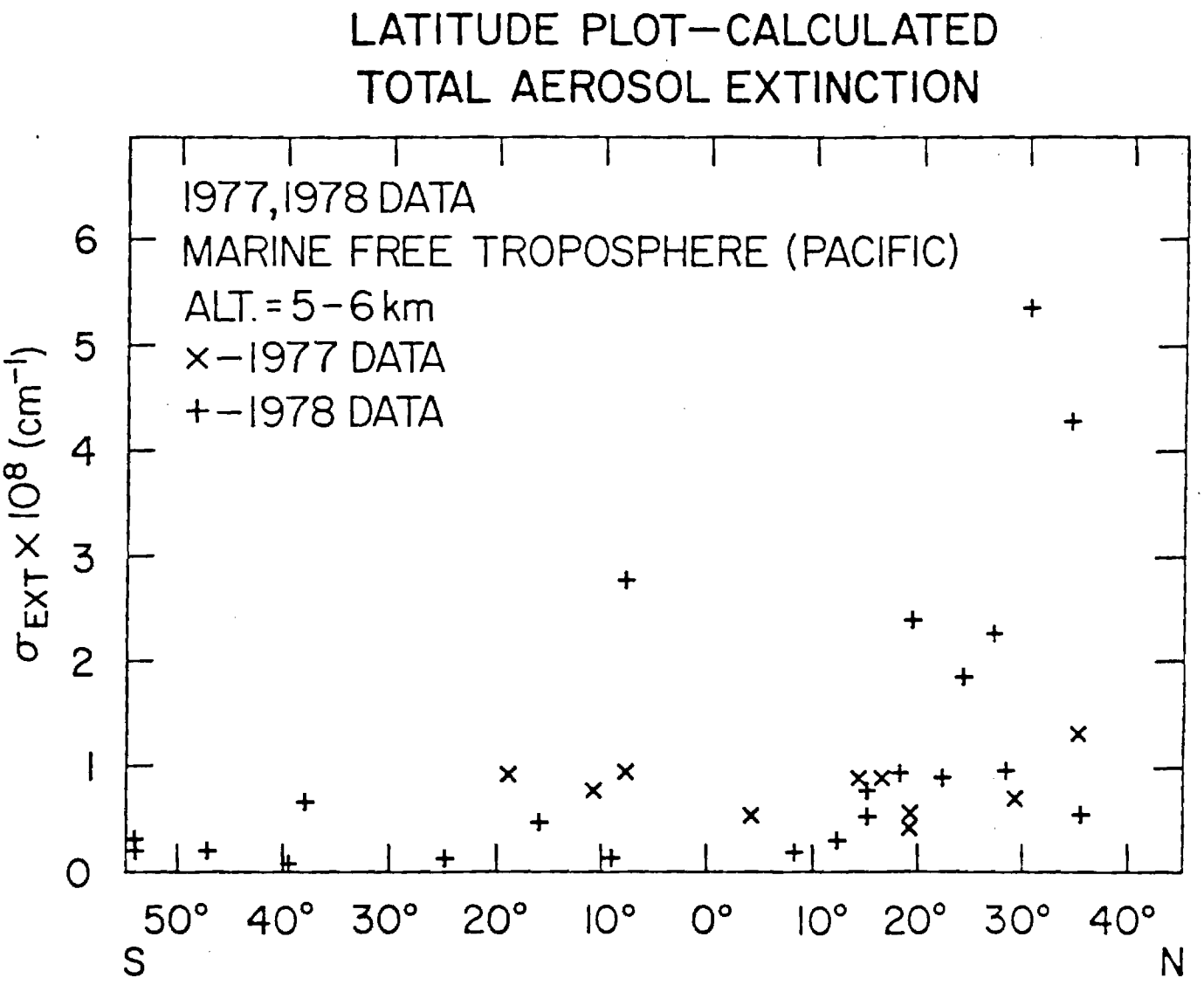
LATITUDE PLOT—CALCULATED
TOTAL AEROSOL EXTINCTION
1977,1978 DATA
MARINE FREE TROPOSPHERE (PACIFIC)
ALT. = 5-6 km
×-1977 DATA
+-1978 DATA
σEXT × 10⁸ (cm⁻¹)
0
1
2
3
4
5
6
50° 40° 30° 20° 10° 0° 10° 20° 30° 40°
S
N

Fig. 19